Statistical wave field theory: Anisotropic wave fields under Robin's boundary condition

Roland Badeau[a]

[a] *Laboratoire Traitement et Communication de l'Information, Télécom Paris, Institut Polytechnique de Paris, Palaiseau 91120, France*

Abstract

The statistical wave field theory mathematically establishes the statistical laws of the solutions to the wave equation in a bounded domain. It provides the closed-form expressions of the power distribution and the correlations of the wave field jointly over time, frequency and space, which hold at high frequency and after many reflections, in terms of the geometry and the specific admittance of the boundary surface. This theory was originally developed in the particular case of mixing rooms, which are characterized by a diffuse wave field, based on the theory of dynamical billiards and on Weyl-like asymptotic laws. Then it was extended to the finite family of special polyhedra, where the wave field is anisotropic, based on a simpler geometric approach related to mathematical crystallography. In this paper, we develop a unified version of the theory dedicated to semi-mixing billiards. In the case of Robin's boundary condition, we show that such wave fields are characterized by a directional reverberation time that is independent of the receiver's position but depends on its orientation, and we provide its closed-form expression, which improves and generalizes Eyring's formula of the reverberation time in ergodic rooms.

Keywords: Statistical physics, wave equation, Helmholtz equation, reverberation

Contents

Email address: roland.badeau@telecom-paris.fr (Roland Badeau)

---

1. Introduction

In the field of room acoustics, it is well known that when waves propagate in a bounded three-dimensional (3D) space, after many reflections on the room boundaries, and at high frequency, their collective behavior becomes stochastic, a physical phenomenon that is known as *late reverberation*. When the room surfaces are rigid, there is no energy absorption, and the wave field is *diffuse* in most common room shapes, which means that its statistics are invariant over space under any translation (it is *stationary*), and any rotation (it is *isotropic*). In the same kind of room shapes, when on the contrary there is energy absorption at the boundary, then the sound power is still uniform in the room, but at fixed frequency it decreases exponentially over time. Late reverberation is thus generally characterized by the *reverberation time*, often denoted T_{60}, which is a function of frequency, and which is defined as the time it takes for the sound pressure level to reduce by 60 dB. During the 20th century, several researchers aimed to characterize mathematically various statistical properties of reverberation, e.g., over time (Moorer, 1979), frequency (Schroeder, 1962), time-frequency (Polack, 1988) and space (Cook *et al.*, 1955). In particular, the reverberation time received special attention, first with the empirical law proposed by Sabine at the end of the 19th century from early experiments, which holds in highly reverberant rooms (Joyce, 1975), then with the modified formula established by Eyring (1930), which holds when the absorption at the boundary is larger, and later with the reverberation theory of Polack (1992).

The main mathematical framework that has been used to model late reverberation, and to establish the closed-form formulas of the reverberation time, is the classical theory of dynamical billiards (Tabachnikov, 1995). Indeed, at high frequency, wave propagation can be approximated in the classical limit by considering the trajectory of rays that undergo successive specular reflections on the domain's boundary, similarly to optical rays (Kuttruff, 2014, Chap. 4). The ray trajectory can then be interpreted as a dynamical billiard that, depending on the boundary geometry, may follow different statistical properties. For instance, a classical billiard is *ergodic* when over time t, the position $\boldsymbol{x}(t) \in V$ and the unit direction vector $\boldsymbol{v}(t) \in \mathcal{S}(0,1)$ of almost every ray trajectory are jointly uniformly distributed in the *phase space* $V \times \mathcal{S}(0,1)$, where the *configuration space* (or *position space*) V is the bounded volume of the billiard, and the *momentum space* $\mathcal{S}(0,1)$ is the unit sphere. In other respects, *mixing* billiards, in addition to being ergodic, are such that two different rays that are arbitrarily close in the phase space at $t = 0$ diverge completely after an asymptotically long elapsed time. Under this assumption and when there is no energy absorption at the boundary, the wave field statistics are independent of the receiver's position and orientation in the room. The wave field is thus stationary and isotropic, so the property of a *diffuse sound field* is induced by the mixing property, which is directly related to the geometry of the room (Polack, 1992). When on the contrary there is energy absorption at the room boundary, then we retrieve the property of a uniform sound power that decreases exponentially over time at fixed frequency, which allows us to define a reverberation time independent of the space position and orientation in the room. In the room acoustics literature, various expressions of the reverberation time in ergodic rooms have been obtained, based on the statistics of the reflections and the mean free path (Joyce, 1978; Polack, 1992; Kuttruff, 2014; Polack, 2025).

Compared to these previous works, in a recent publication (Badeau, 2024), the author of the present paper has opted for a radically different mathematical approach, which proved to be more powerful than the usual methods based on the statistics of the reflections in classical billiards. This innovative approach resulted in a whole new theory called *statistical wave field theory*. This theory aims to establish mathematically the statistical laws of the solutions to the wave equation in a bounded volume. It is the first theory of reverberation that provides the closed-form expression of the power distribution and the correlations of the wave field jointly over time, frequency and space, in terms of the geometry and the specific admittance of the boundary surface. Its prediction of the reverberation time has been verified by experiment (Prinn and Badeau, 2026). Mathematically, the statistical wave field theory is closely related to the Sturm-Liouville theory. Indeed, the solutions to the wave equation in a bounded domain are characterized by the Helmholtz equation that, along with its boundary conditions, forms a particular Sturm-Liouville problem (Al-Gwaiz, 2008). The Sturm-Liouville theory shows that this problem admits a discrete set of solutions, called *eigenmodes* (Kuttruff, 2014, Chap. 3). In several dimensions of space, the density of discrete modes increases with the frequency, in a way that has been investigated mathematically for the first time by Weyl (1911). Since then, a rich literature has been devoted to the study of asymptotic expansions of the modal density as a function of frequency f when $f \to +\infty$, in various space dimensions and various boundary conditions (Arendt *et al.*, 2009). The case of a 3D space and of the real Robin's boundary condition, which is of special interest to us, was addressed by the physicists Balian and Bloch (1970). Their approach was based on the *semiclassical* approximation of quantum physics (Sieber *et al.*, 1995; Brack and Bhaduri, 1997), which also approximates wave propagation by considering the trajectory of rays undergoing specular reflections, as in classical billiards. However, the mathematical treatment of these reflections explicitly depends on Robin's boundary condition, through the *multiple reflection expansion* of the Green's function, used by Balian and Bloch (1970) and Sieber *et al.* (1995). In addition, such rays can pass through the boundary and re-enter the billiard, as illustrated in Balian and Bloch (1972, Fig. 12). Consequently, contrary to the classical theory of dynamical billiards, the semiclassical approximation is able to account for the curvature of the boundary, through the *two-reflection term* of the series expansion of the Green's function, which allowed Balian and Bloch (1970) to pursue the asymptotic expansion of the modal density up to the second order.

Interestingly, up to the first order of this asymptotic expansion, the statistical wave field theory has permitted us to retrieve the previously mentioned statistical properties of reverberation (Badeau, 2024). In addition, based on the mixing assumption, we showed in Badeau (2024) that, if there is no energy absorption at the boundary surface, then the asymptotic expansion of the smoothed modal density directly provides us with a closed-form expression of the *power spectrum* of the stationary wave field. Indeed, because all eigenmodes are uncorrelated and carry on average the same quantity of power when the source position is random, the power spectrum is proportional to the smoothed modal density. If on the contrary there is energy absorption, then the wave field is non-stationary, and the theory proves that its statistics are actually related to the analytic continuation of the smoothed modal density to the domain of complex frequencies. This simple idea has permitted us, in Badeau (2025b), to extend the validity of the statistical wave field theory by exploiting the second order *curvature term* of the asymptotic expansion calculated by Balian and Bloch (1970), which accounts for the impact of a curved boundary surface on the wave field statistics, and which makes the theory predictions hold at lower frequencies.

In references Badeau (2024) and Badeau (2025b), we focused on mixing rooms, in which the reverberation time is independent of the receiver's position and orientation. However, it is well known that in certain non-ergodic room geometries, the reverberation time is still independent of the receiver's position, but it does depend on its orientation (Alary, 2021). In this case, it is sometimes referred to as the *directional reverberation time* (Bilbao and Alary, 2024). The characterization (Nolan *et al.*, 2018; Xu *et al.*, 2022), analysis (Berzborn and Vorländer, 2021; Götz *et al.*, 2023) and synthesis (Alary *et al.*, 2019, 2024) of such *anisotropic* *wave fields* have recently received much attention in the room acoustics community, but curiously, few works have been devoted to the physical modeling of anisotropic reverberation (Meyer-Kahlen and Schlecht, 2024; Drechsler, 2012; Drechsler and Stephenson, 2012).

In room acoustics, the most famous anisotropic room is the *shoebox room*, whose geometric shape is that of a rectangular cuboid. The directional reverberation time in this shoebox room has been investigated in Bilbao and Alary (2024). Then in Badeau (2025c), we have shown the existence of a few other polyhedra whose properties are similar to those of the rectangular cuboid. These so-called *special polyhedra* are neither mixing nor ergodic, but rather *integrable* in the sense of Arnold's theorem (Arnold and Avez, 1989). This means that the Helmholtz equation can be solved in closed-form subject to various boundary conditions (Dirichlet, Neumann, and even Robin in certain cases). Moreover, all the eigenfunctions are trigonometric polynomials. Based on these closed-form solutions, deriving the equations of the statistical wave field theory proved to be much easier than in the mixing case (Badeau, 2025c). This study of the special polyhedra permitted us to take a very important turn in the development of the statistical wave field theory: we have shown that neither the mixing, nor even the ergodic assumptions were actually necessary for this theory to apply, provided that the discrete spectra of these special polyhedra are sufficiently smoothed in the wave vector space.

In Badeau (2026), we then introduced three classes of classical billiards that are referred to as *semi-ergodic*, *weak semi-mixing*, and *strong semi-mixing*, respectively, as these billiards are ergodic, weak mixing, and strong mixing, respectively, in the configuration space, but not necessarily in the momentum space. The general class of 3D semi-ergodic billiards is actually very large: it is not restricted to 3D ergodic billiards and special polyhedra. For instance, it includes all prisms whose basis is a two-dimensional (2D) ergodic billiard (possibly including curved boundaries). It also includes all (possibly non-convex) polyhedra, whether their dihedral angles are rational or irrational multiples of π. These billiards are characterized by a *directional measure* σ defined on the set of unit direction vectors $\mathcal{S}(0, 1)$, which depends on the particular billiard geometry, and whose closed-form expression involves a series expansion over a basis of real spherical harmonics. In addition, the subclass of semi-mixing billiards corresponds to rooms where, through spectral smoothing, at high frequency and after many reflections, the wave field is *wide sense stationary* (WSS) but generally anisotropic when there is no energy absorption, and where the reverberation time is independent of the receiver's position but may depend on its orientation when there is energy absorption. Moreover, the resulting statistics of the anisotropic wave field naturally involve the directional measure σ. In this paper, we address the general case of Robin's boundary condition, which will allow us to provide, for the first time, the general closed-form expression of the directional reverberation time that holds in semi-mixing rooms.

This paper is structured as follows. In the next section, we introduce some acronyms and mathematical notations that will be used in the rest of the paper. Then in Sec. 2, we recall a few fundamental notions regarding wave propagation that are needed to develop the statistical wave field theory. In Sec. 3, we define the three classes of semi-ergodic, weak and strong semi-mixing billiards, and we summarize the properties of their directional measure.

In Sec. 4, we briefly present the Wigner time-frequency distribution that will be used to characterize the second-order properties of non-stationary random processes, and we list the three mathematical assumptions on which the statistical wave field theory relies. In Sec. 5, we recall some key points of the *special* theory dedicated to Neumann's boundary condition. Then in Sec. 6, we present the *general* theory dedicated to Robin's boundary condition. The main results are summarized in Sec. 6.7. Finally, in Sec. 7 we summarize the main contributions of this paper, and we propose a few perspectives for future work.

Acronyms and mathematical notations

Acronyms:

ACF Auto-covariance function

PCF Pseudo-covariance function

RIR Room impulse response

WSS Wide-sense stationary

Mathematical notations:

In this paper, the Greek letter ψ is used to denote *any function of any variables* (we do not use the notation f that is usual in mathematics, because here f denotes the frequency). Therefore, the same letter ψ may denote different functions of different variables in different places of the paper, and it is not supposed to have any special physical meaning.

- $\triangleq$: equal by definition to
- $\mathbb{N}$: set of whole numbers
- $\mathbb{R}$, $\mathbb{C}$: sets of real and complex numbers, respectively
- $\imath = \sqrt{-1}$: imaginary unit
- $\mathbb{R}_-$: set of non-positive real numbers
- $\boldsymbol{x}$ (bold font), z (regular): vector and scalar, respectively
- $[a, b]$: closed interval, including $a, b \in \mathbb{R}$
- $A \backslash B$: relative complement (set difference) of set B in set A
- $A \subseteq B$: A is a subset of B, possibly equal to B
- $\overline{V}$: closure of a subset V of $\mathbb{R}^3$
- $|V|$: Lebesgue measure (volume) of a subset V of $\mathbb{R}^3$
- $\lambda = \frac{1}{|V|}$: mean density of image sources over space
- ∂V: boundary of a subset V of $\mathbb{R}^3$
- $\boldsymbol{n}(\boldsymbol{x})$ where $\boldsymbol{x} \in \partial V$: outward normal to the boundary surface of subset V
- $S(A)$: surface area of a 2-dimensional sub-manifold A of $\mathbb{R}^3$
- $L(C)$: line length of a 1-dimensional sub-manifold C of $\mathbb{R}^3$
- $\|.\|_2$: Euclidean/Hermitian norm of a vector or a function
- $\overline{z}$: complex conjugate of $z \in \mathbb{C}$
- $\mathrm{Re}(z)$ (resp. $\mathrm{Im}(z)$): real (resp. imaginary) part of a complex number $z \in \mathbb{C}$

- $\boldsymbol{x}^\top$: transpose of vector $\boldsymbol{x}$
- $\boldsymbol{x}^H$: conjugate transpose of vector $\boldsymbol{x}$
- $\boldsymbol{I}$: identity matrix
- $A^\perp$: orthogonal complement of set A
- $\mathcal{S}(0,k)$: sphere centered at the origin and of radius k: $\mathcal{S}(0,k) = \{\boldsymbol{k} \in \mathbb{R}^3; \|\boldsymbol{k}\|_2 = k\}$
- $\mathcal{B}(0,k)$: open ball centered at the origin and of radius k: $\mathcal{B}(0,k) = \{\boldsymbol{k} \in \mathbb{R}^3; \|\boldsymbol{k}\|_2 < k\}$
- $L^2(V)$ where V is a Borel subset of $\mathbb{R}^3$: Hilbert space of measurable functions f supported in V, such that $\|f\|_2 = \sqrt{\int_V |f(\boldsymbol{x})|^2 d\boldsymbol{x}} < +\infty$
- $\mathcal{S}(\mathbb{R}^n)$: Schwartz space of smooth functions on $\mathbb{R}^n$, whose derivatives of all orders are rapidly decreasing
- $\langle T|\psi\rangle$: value of the tempered distribution T on the test function $\psi \in \mathcal{S}(\mathbb{R}^n)$
- δ: Dirac delta function
- $H(t)$: Heaviside function: $H(t) = 1\ \forall t > 0$ and $H(t) = 0\ \forall t < 0$
- $\operatorname{sign}(t)$: sign function: $\operatorname{sign}(t) = 1\ \forall t > 0$ and $\operatorname{sign}(t) = -1\ \forall t < 0$
- Jac_ϕ: Jacobian matrix of the multivariate function ϕ
- $\Delta\phi(\boldsymbol{x})$: Laplacian of function $\phi(\boldsymbol{x})$
- $Y_{l,m}(\boldsymbol{u})$ for $l \in \mathbb{N}$, $m \in \{-l, \dots, l\}$, and $\boldsymbol{u} \in \mathcal{S}(0,1)$: real spherical harmonic of degree l and order m;
- 1D direct and inverse Fourier transforms of a function $\psi : \mathbb{R} \to \mathbb{C}$:

$$\begin{aligned} &\widehat{\psi}(f) = \int_{t\in\mathbb{R}} \psi(t) e^{-2\imath\pi f t} dt \\ \text{and} \quad &\psi(t) = \int_{f\in\mathbb{R}} \widehat{\psi}(f) e^{+2\imath\pi f t} df \end{aligned}$$

- 3D direct and inverse Fourier transform of a function $\psi : \mathbb{R}^3 \to \mathbb{C}$:

$$\begin{aligned} &\widehat{\psi}(\boldsymbol{k}) = \int_{\boldsymbol{x}\in\mathbb{R}^3} \psi(\boldsymbol{x}) e^{-2\imath\pi \boldsymbol{k}^\top \boldsymbol{x}} d\boldsymbol{x} \\ \text{and} \quad &\psi(\boldsymbol{x}) = \int_{\boldsymbol{k}\in\mathbb{R}^3} \widehat{\psi}(\boldsymbol{k}) e^{+2\imath\pi \boldsymbol{k}^\top \boldsymbol{x}} d\boldsymbol{k} \end{aligned}$$

- $\mathbb{E}[X]$: expected value of a random variable X
- Covariance of two complex random variables X and Y:

$$\operatorname{cov}[X,Y] = \mathbb{E}[(X - \mathbb{E}[X])\overline{(Y - \mathbb{E}[Y])}]$$

- Pseudo-covariance of two complex random variables X and Y:

$$\operatorname{cov}[X,\overline{Y}] = \mathbb{E}[(X - \mathbb{E}[X])(Y - \mathbb{E}[Y])]$$

- $\boldsymbol{k} \in \mathbb{R}^3$: wave vector related to Neumann's boundary condition
- $\boldsymbol{\kappa} \in \mathbb{C}^3$: wave vector related to Robin's boundary condition
- $\boldsymbol{\mathcal{K}}$: function that assigns $\boldsymbol{\kappa}$ to $\boldsymbol{k}$
- $\kappa = \sqrt{\boldsymbol{\kappa}^\top \boldsymbol{\kappa}} \in \mathbb{C}$: wave number related to Robin's boundary condition
- $k \in \mathbb{R}$: parameter of the Helmholtz equation under Robin's boundary condition characterized by the specific admittance $\widehat{\beta}(\boldsymbol{x}, k)$.

2. Fundamentals of waves revisited

This section summarizes a few fundamental notions regarding wave propagation that are needed in the rest of the paper. Most of these notions are well-known and are described for instance in Morse and Ingard (1968). These and other notions were already presented in more details in Badeau (2024, Sec. III).

2.1. Main definitions

In a connected open domain $V \subseteq \mathbb{R}^3$, the homogeneous wave equation states that

$$\Delta p(\boldsymbol{x}, t) - \frac{1}{c^2}\frac{\partial^2 p(\boldsymbol{x}, t)}{\partial t^2} = 0, \tag{1}$$

where $p(\boldsymbol{x}, t)$ is the wave amplitude at position $\boldsymbol{x} \in V$ and time $t \in \mathbb{R}$, Δ is the Laplacian, and c is the propagation speed of the wave. Applying the 1D Fourier transform w.r.t. time to Eq. (1) yields the Helmholtz equation:

$$\Delta\phi(\boldsymbol{x}) + 4\pi^2 k^2 \phi(\boldsymbol{x}) = 0, \tag{2}$$

where the scalar $k = \frac{f}{c}$ is the *wave number* and f denotes the frequency. We note that any solution ϕ to Eq. (2) is an eigenfunction of the Laplace operator, of eigenvalue $-4\pi^2 k^2$.

Given a punctual source position $\boldsymbol{x}_0 \in V$ and a space position $\boldsymbol{x} \in V$, we define the *source response* p as the unique causal solution to the following inhomogeneous wave equation: $\forall t \in \mathbb{R}$,

$$\Delta p(\boldsymbol{x}, \boldsymbol{x}_0, t) - \frac{1}{c^2}\frac{\partial^2 p(\boldsymbol{x}, \boldsymbol{x}_0, t)}{\partial t^2} = -\delta(\boldsymbol{x} - \boldsymbol{x}_0)\dot{\delta}(t). \tag{3}$$

Note that the right member of Eq. (3) involves the derivative of a Dirac delta function over time, in order to account for the fact that the response of a physical source is always zero at the zero frequency (Morse and Ingard, 1968, Chap. 7). Replacing the derivative $\dot{\delta}(t)$ with $\delta(t)$ in Eq. (3) would lead to the usual definition of the *room impulse response* (RIR) $h(\boldsymbol{x}, \boldsymbol{x}_0, t)$ in room acoustics, which is the causal Green's function of the wave equation [Eq. (1)]. Therefore, the RIR h is the unique causal primitive of the source response p defined in Eq. (3).

2.2. Green's function

Given a punctual source position $\boldsymbol{x}_0 \in V$ and a space position $\boldsymbol{x} \in V$, a Green's function G of the Helmholtz equation is a particular solution to the following inhomogeneous Helmholtz equation:

$$\Delta G(\boldsymbol{x}, \boldsymbol{x}_0, k) + 4\pi^2 k^2 G(\boldsymbol{x}, \boldsymbol{x}_0, k) = -\delta(\boldsymbol{x} - \boldsymbol{x}_0). \tag{4}$$

The inverse 1D Fourier transform of G w.r.t. frequency $f = ck$,

$$g(\boldsymbol{x}, \boldsymbol{x}_0, t) = \int_{f \in \mathbb{R}} G(\boldsymbol{x}, \boldsymbol{x}_0, \tfrac{f}{c})\, e^{2\imath\pi f t} df, \tag{5}$$

is such that its time derivative $\dot{g}(\boldsymbol{x}, \boldsymbol{x}_0, t)$ is a solution to Eq. (3). However, depending on the choice of a particular solution G to Eq. (4), the function $\dot{g}(\boldsymbol{x}, \boldsymbol{x}_0, t)$ may not be causal, so in general $\dot{g}(\boldsymbol{x}, \boldsymbol{x}_0, t)$ differs from the causal source response $p(\boldsymbol{x}, \boldsymbol{x}_0, t)$ by a function that is a solution to the homogeneous wave equation [Eq. (1)].

2.3. B-function

In the case of a connected domain $V \subset \mathbb{R}^3$ with boundaries, any Green's function $G(\boldsymbol{x}, \boldsymbol{x}_0, k)$ can generally be analytically continued in a mathematical vicinity $\mathcal{D}$ of V that depends on the domain's geometry and the boundary condition. In some cases, this extension holds in the full space $\mathcal{D} = \mathbb{R}^3$. The B-function on $\mathcal{D} \subseteq \mathbb{R}^3$ is then defined as:

$$B(\boldsymbol{y}, \boldsymbol{x}_0, k) = -\left(\Delta G(\boldsymbol{y}, \boldsymbol{x}_0, k) + 4\pi^2 k^2 G(\boldsymbol{y}, \boldsymbol{x}_0, k)\right). \tag{6}$$

By definition of the Green's function G in Eq. (4), the restriction of the B-function to V is $\delta(\boldsymbol{y} - \boldsymbol{x}_0)$.

2.4. Robin's boundary condition

Let us consider a connected domain $V \subset \mathbb{R}^3$, whose boundary ∂V is a Lipschitz continuous 2D manifold (i.e., ∂V is locally the graph of a Lipschitz function). The boundary ∂V is characterized by the *specific admittance* $\widehat{\beta}(\boldsymbol{x}, k) \in \mathbb{C}$, which is an essentially bounded function of the position $\boldsymbol{x} \in \partial V$. Then Robin's boundary condition of the Helmholtz equation [Eq. (2)] states that

$$\forall \boldsymbol{x} \in \partial V,\ \frac{\partial \varphi(\boldsymbol{x}, k)}{\partial \boldsymbol{n}(\boldsymbol{x})} + 2\imath\pi k \widehat{\beta}(\boldsymbol{x}, k)\varphi(\boldsymbol{x}, k) = 0, \tag{7}$$

where $\frac{\partial}{\partial \boldsymbol{n}(\boldsymbol{x})}$ denotes partial differentiation in the direction of the outward normal $\boldsymbol{n}(\boldsymbol{x})$ to the boundary surface at $\boldsymbol{x}$. In the case of *non-rigid* surfaces, which absorb a part of the energy of the incident wave, $\widehat{\beta}(\boldsymbol{x}, k)$ is complex and the real part of $\widehat{\beta}(\boldsymbol{x}, k)$ is positive. Then we proved in Badeau (2025a) that when the domain V is bounded, the set of eigenfunctions and generalized eigenfunctions of the complex Robin Laplacian is discrete and can be chosen to form a pseudo-orthonormal *Abel basis with brackets* of the Hilbert space $L^2(V)$, a notion that is defined in Badeau (2025a, Sec. III A). However, when there is no energy absorption, $\widehat{\beta}(\boldsymbol{x}, k)$ is purely imaginary, the Robin Laplacian is self-adjoint, and the set of eigenfunctions forms an orthonormal basis of $L^2(V)$. Also note that when $k = 0$, Eq. (7) reduces to Neumann's boundary condition.

In the rest of this paper, the wave vector will be denoted $\boldsymbol{\kappa}$ in the case of Robin's boundary condition, instead of notation $\boldsymbol{k}$ that will be dedicated to Neumann's boundary condition, in order to avoid any confusion, especially in Sec. 6, where the two notations will coexist. In the same way, again in the Robin case, the wave number will be denoted $\kappa \triangleq \sqrt{\boldsymbol{\kappa}^\top \boldsymbol{\kappa}}$, and should not be confused with the parameter k of the Helmholtz equation [Eq. (2)] under the boundary condition in Eq. (7).

3. Semi-ergodic billiards

In this section, the three classes of semi-ergodic billiards mentioned in Sec. 1 are characterized mathematically. In the definitions that follow, $(\boldsymbol{x}(t), \boldsymbol{v}(t)) \in V \times \mathcal{S}(0,1)$ denotes the value in the phase space, at time $t \geq 0$, of the ray trajectory that starts at initial position $\boldsymbol{x}(0) = \boldsymbol{x} \in V$ and initial direction $\boldsymbol{v}(0) = \boldsymbol{v} \in \mathcal{S}(0,1)$. In addition, $\sigma(.|\boldsymbol{v})$ denotes a probability measure over $\mathcal{S}(0,1)$, which will be referred to as the *directional measure*.

Definition 1 (Semi-ergodic billiards). *A classical billiard is* semi-ergodic *if and only if, for almost every ray trajectory and for any continuous function ψ defined on the phase space $V \times \mathcal{S}(0,1)$,*

$$\lim_{T\to+\infty} \frac{1}{T}\int_0^T \psi(\boldsymbol{x}(t),\boldsymbol{v}(t))\,dt = \int_{\boldsymbol{u}\in\mathcal{S}(0,1)}\int_{\boldsymbol{y}\in V} \psi(\boldsymbol{y},\boldsymbol{u})\,\frac{d\boldsymbol{y}}{|V|}\,d\sigma(\boldsymbol{u}|\boldsymbol{v}). \tag{8}$$

Definition 2 (Weak semi-mixing billiards). *A classical billiard is* weak semi-mixing *if and only if, for any continuous function ψ and measurable function ϕ defined on the phase space $V \times \mathcal{S}(0,1)$,*

$$\begin{aligned}&\lim_{T\to+\infty} \frac{1}{T}\int_0^T \Big| \int_{\boldsymbol{v}\in\mathcal{S}(0,1)}\int_{\boldsymbol{x}\in V}\\ &\Big(\psi(\boldsymbol{x}(t),\boldsymbol{v}(t)) - \int_{\boldsymbol{u}\in\mathcal{S}(0,1)}\int_{\boldsymbol{y}\in V}\psi(\boldsymbol{y},\boldsymbol{u})\,\frac{d\boldsymbol{y}}{|V|}d\sigma(\boldsymbol{u}|\boldsymbol{v})\Big)\,\phi(\boldsymbol{x},\boldsymbol{v})\,\frac{d\boldsymbol{x}}{|V|}\frac{dS(\boldsymbol{v})}{4\pi}\Big|dt = 0.\end{aligned} \tag{9}$$

Definition 3 (Strong semi-mixing billiards). *A classical billiard is* strong semi-mixing *(or* semi-mixing*) if and only if, for any continuous function ψ and measurable function ϕ defined on the phase space $V \times \mathcal{S}(0,1)$,*

$$\begin{aligned}&\lim_{t\to+\infty}\int_{\boldsymbol{v}\in\mathcal{S}(0,1)}\int_{\boldsymbol{x}\in V}\psi(\boldsymbol{x}(t),\boldsymbol{v}(t))\phi(\boldsymbol{x},\boldsymbol{v})\,\frac{d\boldsymbol{x}}{|V|}\frac{dS(\boldsymbol{v})}{4\pi}\\ =\;&\int_{\boldsymbol{v}\in\mathcal{S}(0,1)}\Big(\int_{\boldsymbol{u}\in\mathcal{S}(0,1)}\int_{\boldsymbol{y}\in V}\psi(\boldsymbol{y},\boldsymbol{u})\,\frac{d\boldsymbol{y}}{|V|}d\sigma(\boldsymbol{u}|\boldsymbol{v})\Big)\int_{\boldsymbol{x}\in V}\phi(\boldsymbol{x},\boldsymbol{v})\,\frac{d\boldsymbol{x}}{|V|}\frac{dS(\boldsymbol{v})}{4\pi}.\end{aligned} \tag{10}$$

Note that all strong semi-mixing billiards are weak semi-mixing, and all weak semi-mixing billiards are semi-ergodic. When the directional measure is isotropic (i.e., $d\sigma(\boldsymbol{u}|\boldsymbol{v}) = \frac{1}{4\pi}\,dS(\boldsymbol{u})\ \forall \boldsymbol{v}\in\mathcal{S}(0,1)$), we retrieve the usual definitions of ergodic, weak mixing, and strong mixing billiards, respectively. When on the contrary, the directional measure is not isotropic, there are known examples of semi-ergodic and weak semi-mixing billiards. For instance, the mathematical results presented in Arana-Herrera *et al.* (2025) can be extended in 3D to show that not every, but *almost every* rational polyhedron (i.e., whose dihedral angles are rational multiples of π), is not weak mixing, but rather weak *semi*-mixing. The rare exceptions include the set of almost integrable polyhedra, which includes the four *special polyhedra* (Badeau, 2025c), which are semi-ergodic, but not weak semi-mixing.

Let us now investigate the classical properties of semi-ergodic billiards introduced in Definition 1. Equation (8) shows that the configuration space V and the momentum space $\mathcal{S}(0,1)$ are explored independently by almost every ray trajectory. Moreover, V is explored uniformly over time, and $\mathcal{S}(0,1)$ is explored according to the probability measure σ. More precisely, if $\boldsymbol{v} = \boldsymbol{v}(0)$ is the initial direction of the ray trajectory, then over time t the ray explores the directions $\boldsymbol{u}\in\mathcal{S}(0,1)$ according to the probability measure $d\sigma(\boldsymbol{u}|\boldsymbol{v})$.

In Badeau (2026, Sec. III), the directional measure σ was characterized as follows. For all $l\in\mathbb{N}$, let $\boldsymbol{Y}_l$ denote the $(2l+1)$-dimensional column vector of coefficients $Y_{l,m}$, where $\forall m\in\{-l,\dots,l\}$, $Y_{l,m}$ denotes the real spherical harmonic of degree l and order m (Courant and Hilbert, 2004). Then $\forall l\in\mathbb{N}$, let $\boldsymbol{A}_l$ be the $(2l+1)\times(2l+1)$ real symmetric positive semidefinite matrix

$$\boldsymbol{A}_l = \lambda\int_{\partial V}\Big(\boldsymbol{I} - \Big(\int_{\boldsymbol{u}\in\mathcal{S}(0,1)}\boldsymbol{Y}_l(\boldsymbol{u})\boldsymbol{Y}_l\left(\boldsymbol{u}-2(\boldsymbol{n}(\boldsymbol{s})^\top\boldsymbol{u})\boldsymbol{n}(\boldsymbol{s})\right)^\top dS(\boldsymbol{u})\Big)\Big)dS(\boldsymbol{s}), \tag{11}$$

where $\boldsymbol{I}$ denotes the identity matrix. Then $\forall \boldsymbol{v} \in \mathcal{S}(0,1)$, the directional measure $\sigma(S|\boldsymbol{v})$ of any measurable subset S of the unit sphere $\mathcal{S}(0,1)$ is expressed as

$$\sigma(S|\boldsymbol{v}) = \lim_{L\to+\infty} \int_{\boldsymbol{u}\in S} \sigma_L(\boldsymbol{u},\boldsymbol{v}) dS(\boldsymbol{u}), \tag{12}$$

where $\forall L \in \mathbb{N}$,

$$\sigma_L(\boldsymbol{u},\boldsymbol{v}) = \sum_{l=0}^{L} \boldsymbol{Y}_l(\boldsymbol{v})^\top \mathrm{Proj}_{\mathrm{Ker}(\boldsymbol{A}_l)} \boldsymbol{Y}_l(\boldsymbol{u}). \tag{13}$$

Since the series expansion over spherical harmonics in Eq. (13) is truncated to degree L, $\boldsymbol{u} \mapsto \sigma_L(\boldsymbol{u},\boldsymbol{v})$ can be interpreted as a smooth density function over $\mathcal{S}(0,1)$, which can equivalently be obtained by smoothing the (possibly discrete) directional measure σ defined in Eq. (12), over the set of unit direction vectors $\boldsymbol{u} \in \mathcal{S}(0,1)$. Finally, we made in Badeau (2026, Sec. III) the following remarks:

Remark 1 (Properties of function σ_L and measure σ)**.** *The bivariate function $\sigma_L(\boldsymbol{u},\boldsymbol{v})$ in Eq. (13) is a real-valued analytic function of $\boldsymbol{u}$ and $\boldsymbol{v}$. It is symmetric (i.e., $\sigma_L(\boldsymbol{v},\boldsymbol{u}) = \sigma_L(\boldsymbol{u},\boldsymbol{v})$), even (i.e., $\sigma_L(-\boldsymbol{u},-\boldsymbol{v}) = \sigma_L(\boldsymbol{u},\boldsymbol{v})$), and such that $\sigma_L(\boldsymbol{u},\boldsymbol{u}) \geq 0$. When $L \to +\infty$, σ in Eq. (12) is indeed a measure (i.e., $\sigma(S|\boldsymbol{v}) \geq 0 \ \forall S \subset \mathcal{S}(0,1)$). Finally, $\forall \boldsymbol{v} \in \mathcal{S}(0,1)$, $\sigma\left(\mathcal{S}(0,1)|\boldsymbol{v}\right) = 1$, and in the same way, $\forall L \in \mathbb{N}$, $\int_{\boldsymbol{u}\in\mathcal{S}(0,1)} \sigma_L\left(\boldsymbol{u},\boldsymbol{v}\right) dS(\boldsymbol{u}) = 1$. Therefore, the directional measure σ and the smooth density function σ_L sum to one on $\mathcal{S}(0,1)$, like a probability measure and a probability density function, respectively.*

Remark 2 (Ergodic billiards)**.** *In the particular case of ergodic billiards, Eqs. (12) and (13) yield $\forall \boldsymbol{u},\boldsymbol{v} \in \mathcal{S}(0,1)$,*

$$d\sigma(\boldsymbol{u}|\boldsymbol{v}) = \tfrac{1}{4\pi}\, dS(\boldsymbol{u}). \tag{14}$$

Remark 3 (Special polyhedra)**.** *In the case of special polyhedra, Eqs. (12) and (13) are equivalent to*

$$\sigma(\boldsymbol{u}|\boldsymbol{v}) = \tfrac{1}{|\mathrm{D}_{n\mathrm{h}}|} \sum_{\boldsymbol{Q}\in\mathrm{D}_{n\mathrm{h}}} \delta_{\mathcal{S}(0,1)}(\boldsymbol{u}, \boldsymbol{Q}\,\boldsymbol{v}),$$

where $\delta_{\mathcal{S}(0,1)}$ denotes the Dirac distribution on the unit sphere, and $\mathrm{D}_{n\mathrm{h}}$ is the finite dihedral point group of isometries $\boldsymbol{Q}$ generated by all the reflections through the polyhedron's faces.

4. Fundamentals of the statistical wave field theory

4.1. Wigner distribution

When there is energy absorption at the domain's boundary, the causal source response $p(\boldsymbol{x},\boldsymbol{x}_0,t)$, introduced in Sec. 2.1, which is a function of the space position $\boldsymbol{x} \in V$, the source position $\boldsymbol{x}_0 \in V$, and time $t \in \mathbb{R}$, is modeled as a non-stationary random process in Sec. 6, due to the exponential damping of the eigenmodes over time. From Sec. 5, we will consider a random process $q(\boldsymbol{x},\boldsymbol{x}_0,t)$ that is equal to $p(\boldsymbol{x},\boldsymbol{x}_0,t)$ for $t \geq 0$ [see Eq. (35)]. In signal processing, the standard tool for characterizing the second-order statistics of a non-stationary random process is the *Wigner distribution* (Cohen, 1989), also known as the Wigner-Ville distribution, which describes how the power of this random process is distributed in the time-frequency plane. Let

$$\Gamma_q(\boldsymbol{x}_1, \boldsymbol{x}_2, \boldsymbol{x}_0, t_1, t_2) = \mathrm{cov}[q(\boldsymbol{x}_1, \boldsymbol{x}_0, t_1), q(\boldsymbol{x}_2, \boldsymbol{x}_0, t_2)] \tag{15}$$

denote the *auto-covariance function* (ACF) of the random process $q(\boldsymbol{x}, \boldsymbol{x}_0, t)$. Its *cross-Wigner distribution* W_q is then defined as follows: $\forall \boldsymbol{x}_1, \boldsymbol{x}_2, \boldsymbol{x}_0 \in V$, $\forall f, t \in \mathbb{R}$,

$$W_q(\boldsymbol{x}_1, \boldsymbol{x}_2, \boldsymbol{x}_0, f, t) = \int_{\mathbb{R}} \Gamma_q(\boldsymbol{x}_1, \boldsymbol{x}_2, \boldsymbol{x}_0, t + \tfrac{\tau}{2}, t - \tfrac{\tau}{2})\, e^{-2\imath\pi f \tau} d\tau. \tag{16}$$

The cross-Wigner distribution $W_q(\boldsymbol{x}_1, \boldsymbol{x}_2, \boldsymbol{x}_0, f, t)$ in Eq. (16) can be interpreted as the covariance of the random process q between two positions $\boldsymbol{x}_1$ and $\boldsymbol{x}_2$, at fixed frequency f and time t, when the source is located at $\boldsymbol{x}_0$.

In applications, it may be more convenient to consider the cross-Wigner distribution of the RIR $h(\boldsymbol{x}, \boldsymbol{x}_0, t)$ rather than that of the random process $q(\boldsymbol{x}, \boldsymbol{x}_0, t)$. In Badeau (2026, Sec. IV A), we showed that the general relationship between $W_q(\boldsymbol{x}_1, \boldsymbol{x}_2, \boldsymbol{x}_0, f, t)$ and $W_h(\boldsymbol{x}_1, \boldsymbol{x}_2, \boldsymbol{x}_0, f, t)$ is

$$W_q(\boldsymbol{x}_1, \boldsymbol{x}_2, \boldsymbol{x}_0, f, t) = \left(4\pi^2 f^2 + \tfrac{1}{4}\tfrac{\partial^2}{\partial t^2}\right) W_h(\boldsymbol{x}_1, \boldsymbol{x}_2, \boldsymbol{x}_0, f, t). \tag{17}$$

4.2. Mathematical assumptions

The statistical wave field theory relies on three mathematical assumptions:

- Assumption 1: the source's position is a random variable uniformly distributed in V;
- Assumption 2: the frequency f (or equivalently the wave number k) is large;
- Assumption 3: the mean and pseudo-covariances of the B-function are stationary.

These three assumptions are directly related to the properties of semi-mixing billiards introduced in Definition 3. We refer the reader to Badeau (2026, Sec. IV B) for a detailed explanation, in the particular case of Neumann's boundary condition. Here, in the general case of Robin's boundary condition, we will just add that the second assumption is directly related to the semiclassical approximation of quantum physics, in the way it is formulated in Balian and Bloch (1970) and Sieber *et al.* (1995), i.e., $\kappa \to +\infty$ but $\frac{k\widehat{\beta}(\boldsymbol{x},k)}{\kappa}$ is an independent parameter that does not tend to zero.

Regarding the third assumption, the B-function is assumed to be a complex pseudo-stationary random process, which means that both its mean $\mu_B(k) = \mathbb{E}[B(\boldsymbol{y}, \boldsymbol{x}_0, k)]$ and its pseudo-covariances $\mathrm{cov}[B(\boldsymbol{y}+\boldsymbol{z}, \boldsymbol{x}_0, k), \overline{B(\boldsymbol{y}, \boldsymbol{x}_0, k)}]$ are well-defined and do not depend on $\boldsymbol{y}$. Its stationary first and second order statistics are then characterized by the mean $\mu_B(k) = \lambda$ (as proved in Badeau (2024, Sec. IV D 2)), the *pseudo-covariance function* (PCF) $J_B(\boldsymbol{z}, k) \triangleq \mathrm{cov}[B(\boldsymbol{y}+\boldsymbol{z}, \boldsymbol{x}_0, k), \overline{B(\boldsymbol{y}, \boldsymbol{x}_0, k)}]$, and its 3D Fourier transform, the anisotropic *pseudo spectral measure* $\widehat{J}_B(\mathcal{K}, k)$, whose closed-form expression will be established in Sec. 6.1.

5. Special statistical wave field theory

In Badeau (2026, Sec. V), we showed that in the case of Neumann's boundary condition, the Green's function $G(\boldsymbol{x}, \boldsymbol{x}_0, k)$ is a WSS random process over space, of mean

$$\mu_G(k) = -\frac{\lambda}{4\pi^2 k^2}, \tag{18}$$

which admits the following spectral representation[1]:

$$G(\boldsymbol{x}, \boldsymbol{x}_0, k) = \mu_G(k) + \int_{\boldsymbol{k}\in\mathbb{R}^3} \int_{\boldsymbol{s}\in\overline{V}} \frac{e^{2\imath\pi \boldsymbol{k}^\top(\boldsymbol{x}-\boldsymbol{s})}}{4\pi^2(\|\boldsymbol{k}\|_2^2 - k^2)} d\widehat{\xi}_L(\boldsymbol{k}, \boldsymbol{s}), \tag{19}$$

where notation L refers to the truncation of the series expansion over spherical harmonics introduced in Sec. 3 to a finite degree L. In Eq. (19), which has the same form as Badeau (2024, Eq. (81)), $\widehat{\xi}_L$ is a centered complex random measure with uncorrelated increments $d\widehat{\xi}_L(\boldsymbol{k}, \boldsymbol{s})$ on $\mathbb{R}^3 \times \overline{V}$, which is Hermitian symmetric w.r.t. $\boldsymbol{k}$, such that for any Borel sets $\mathcal{K} \subset \mathbb{R}^3$ and $\mathcal{V} \subset \overline{V}$,

$$\mathbb{E}\left[\left(\widehat{\xi}_L(\mathcal{K}, \mathcal{V})\right)^2\right] = 0 \text{ and } \mathbb{E}\left[\left|\widehat{\xi}_L(\mathcal{K}, \mathcal{V})\right|^2\right] = \widehat{\Lambda}_L(\mathcal{K}, \mathcal{V}), \tag{20}$$

where the spectral measure $\widehat{\Lambda}_L$ on $\mathbb{R}^3 \times \overline{V}$ was expressed in Eq. (B6) in Badeau (2026, Appendix B):

$$\begin{aligned} \widehat{\Lambda}_L(\mathcal{K}, \mathcal{V}) = \; & \lambda^2\Big(|\mathcal{K}||\mathcal{V}| + \tfrac{1}{4} \int_{\boldsymbol{k}\in\mathcal{K}} \int_{\boldsymbol{s}\in\mathcal{V}\cap\partial V} \int_{\boldsymbol{u}\in\mathcal{S}(0,1)} \\ & \delta\left(\boldsymbol{u}^\top \boldsymbol{k}\right) \sigma_L(\boldsymbol{u}, \boldsymbol{n}(\boldsymbol{s}))\, dS(\boldsymbol{u})\, dS(\boldsymbol{s})\, d\boldsymbol{k}\Big), \end{aligned} \tag{21}$$

and function σ_L was defined in Eq. (13). In the same way, we showed that the B-function is a WSS random process of mean $\mu_B = \lambda$, and of power spectrum

$$\widehat{\Gamma}_L(\boldsymbol{k}) = \lambda\Big(1 + \tfrac{\lambda}{4} \int_{\boldsymbol{s}\in\partial V} \Big(\int_{\boldsymbol{u}\in\mathcal{S}(0,1)} \delta\left(\boldsymbol{u}^\top \boldsymbol{k}\right) \sigma_L(\boldsymbol{u}, \boldsymbol{n}(\boldsymbol{s}))\, dS(\boldsymbol{u})\Big) dS(\boldsymbol{s})\Big), \tag{22}$$

which is such that for any Borel set $\mathcal{K} \subset \mathbb{R}^3$,

$$\int_{\boldsymbol{k}\in\mathcal{K}} \widehat{\Gamma}_L(\boldsymbol{k}) d\boldsymbol{k} = \widehat{\Lambda}_L(\mathcal{K}, \overline{V}) \tag{23}$$

(Badeau, 2026, Eq. (B7) in Appendix B). From the spectral representation of the Green's function in Eq. (19), we were then able to deduce in Badeau (2026, Sec. V D) the (cross-)Wigner distribution of the WSS source response, which was expressed as a function of the power spectrum $\widehat{\Gamma}_L(\boldsymbol{k})$ in Eq. (22).

[1] Actually, the expression of the spectral representation in Eq. (19) was simplified in Badeau (2026, Sec. V), by introducing the random measure $d\widehat{B}_L(\boldsymbol{k}) = \int_{\boldsymbol{s}\in\overline{V}} d\widehat{\xi}_L(\boldsymbol{k}, \boldsymbol{s})$, and by modifying the origin of the coordinate system.

6. General statistical wave field theory

The main purpose of the general statistical wave field theory is to show that Robin's boundary condition induces a non-linear distortion of the real wave vectors $\boldsymbol{k}$ related to Neumann's boundary condition. In particular, when there is energy absorption at the boundary (i.e., when $\mathrm{Re}(\widehat{\beta}) > 0$), the distorted Robin's wave vectors $\boldsymbol{\kappa}$ are complex, the room response $p(\boldsymbol{x}, \boldsymbol{x}_0, t)$ to a punctual source can be decomposed onto a set of plane waves $e^{2\imath\pi\left(\boldsymbol{\kappa}^\top \boldsymbol{x} + c\kappa t\right)}$ and their complex conjugates [Eqs. (35) and (36)], where $\kappa \triangleq \sqrt{\boldsymbol{\kappa}^\top \boldsymbol{\kappa}}$ denotes the complex square root of $\boldsymbol{\kappa}^\top \boldsymbol{\kappa} \in \mathbb{C}$ with positive imaginary part (these plane waves have direction $\mathrm{Re}(\boldsymbol{\kappa})$, frequencies $\pm c\,\mathrm{Re}(\kappa)$ and temporal attenuation coefficient $c\,\mathrm{Im}(\kappa) > 0$). In addition, the general statistical wave field theory provides the closed-form expression of the non-linear distortion that transforms the Neumann's wave vectors $\boldsymbol{k}$ into the corresponding Robin's wave vectors $\boldsymbol{\kappa}$ [Eq. (39)].

6.1. Asymptotic expansion of the pseudo spectral measure

At finite degree L, the closed-form expression of the anisotropic pseudo spectrum $\widehat{J}_L$ is derived in Appendix A:

$$\begin{aligned} \widehat{J}_L(\boldsymbol{\kappa}, k) = \;& \lambda\Big(1 + \tfrac{\lambda}{4\pi} \int_{\boldsymbol{s}\in\partial V} \int_{\boldsymbol{u}\in\mathcal{S}(0,1)} \\ & \Big(\pi\left(1 + 2\,\mathrm{sign}(\mathrm{Im}(k\,\widehat{\beta}(\boldsymbol{s}, k)))\right) \delta\left(\boldsymbol{u}^\top \boldsymbol{\kappa}\right) - \tfrac{\imath}{\boldsymbol{u}^\top\boldsymbol{\kappa} + k\widehat{\beta}(\boldsymbol{s},k)} + \tfrac{\imath}{\boldsymbol{u}^\top\boldsymbol{\kappa} - k\widehat{\beta}(\boldsymbol{s},k)}\Big) \\ & \times \sigma_L(\boldsymbol{u}, \boldsymbol{n}(\boldsymbol{s})) dS(\boldsymbol{u})\, dS(\boldsymbol{s})\Big), \end{aligned} \tag{24}$$

where function σ_L was defined in Eq. (13).

In the same way as in Badeau (2026, Sec. V A), it can be easily proved that if $k\widehat{\beta}(\boldsymbol{s}, k) \notin \mathbb{R}$, then the pseudo spectrum $\widehat{J}_L(\boldsymbol{\kappa}, k)$ is an analytic function of $\boldsymbol{\kappa}$ on $\mathbb{R}^3 \backslash \{\boldsymbol{0}\}$, therefore function $\boldsymbol{\kappa} \mapsto \widehat{J}_L(\boldsymbol{\kappa}, k)$ can be analytically continued in a vicinity of $\mathbb{R}^3 \backslash \{\boldsymbol{0}\}$ in $\mathbb{C}^3$. When $L \to +\infty$, the sequence of analytic functions $\widehat{J}_L(\boldsymbol{\kappa}, k)$ converges in the sense of distributions to the pseudo spectral measure $\widehat{J}_B$ of the WSS B-function, which is defined as $\forall \mathcal{K} \subset \mathbb{R}^3$,

$$\begin{aligned} \widehat{J}_B(\mathcal{K}, k) = \;& \int_{\boldsymbol{\kappa}\in\mathcal{K}} \lambda\Big(1 + \tfrac{\lambda}{4\pi} \int_{\boldsymbol{s}\in\partial V} \int_{\boldsymbol{u}\in\mathcal{S}(0,1)} \\ & \Big(\pi\left(1 + 2\,\mathrm{sign}(\mathrm{Im}(k\,\widehat{\beta}(\boldsymbol{s}, k)))\right) \delta\left(\boldsymbol{u}^\top \boldsymbol{\kappa}\right) - \tfrac{\imath}{\boldsymbol{u}^\top\boldsymbol{\kappa} + k\widehat{\beta}(\boldsymbol{s},k)} + \tfrac{\imath}{\boldsymbol{u}^\top\boldsymbol{\kappa} - k\widehat{\beta}(\boldsymbol{s},k)}\Big) \\ & \times d\sigma(\boldsymbol{u}|\boldsymbol{n}(\boldsymbol{s}))\, dS(\boldsymbol{s})\Big) d\boldsymbol{\kappa}, \end{aligned} \tag{25}$$

where the directional measure σ was expressed in Eq. (12). Note that the pseudo spectral measure $\widehat{J}_B$ in Eq. (25) is actually a complex measure when the specific admittance $\widehat{\beta}$ is not purely imaginary.

6.2. Wave vectors distortion

In Appendix B, it is proved that the power spectrum $\widehat{\Gamma}_L(\boldsymbol{k})$ in Eq. (22) and the analytic continuation of the pseudo spectrum $\widehat{J}_L(\boldsymbol{\kappa}, k)$ in Eq. (24) are related through the equation

$$\widehat{\Gamma}_L(\boldsymbol{k}) = \widehat{J}_L(\boldsymbol{\mathcal{K}}_L(\boldsymbol{k}, k), k) \det\left(\mathrm{Jac}_{\boldsymbol{\mathcal{K}}_L}(\boldsymbol{k}, k)\right), \tag{26}$$

where $\text{Jac}_{\boldsymbol{\mathcal{K}}_L}(\boldsymbol{k}, k)$ denotes the Jacobian matrix of the wave vectors distortion function $\boldsymbol{\mathcal{K}}_L : \mathbb{R}^3 \times \mathbb{C} \to \mathbb{C}^3$, which, asymptotically at high frequency, satisfies the implicit equation:

$$\boldsymbol{\mathcal{K}}_L(\boldsymbol{k}, k) = \boldsymbol{k} + \imath \, \tfrac{\lambda}{4\pi} \int_{\boldsymbol{s} \in \partial V} \left(\int_{\boldsymbol{u} \in \mathcal{S}(0,1)} \boldsymbol{u} \, \ln \left(\tfrac{\boldsymbol{u}^\top \boldsymbol{\mathcal{K}}_L(\boldsymbol{k},k) + k \, \widehat{\beta}(\boldsymbol{s},k)}{\boldsymbol{u}^\top \boldsymbol{\mathcal{K}}_L(\boldsymbol{k},k) - k \, \widehat{\beta}(\boldsymbol{s},k)} \right) \sigma_L(\boldsymbol{u}, \boldsymbol{n}(\boldsymbol{s})) \, dS(\boldsymbol{u}) \right) dS(\boldsymbol{s}). \tag{27}$$

Equation (27) thus holds as a first order asymptotic expansion when $\|\boldsymbol{k}\|_2 \to +\infty$. Function $\boldsymbol{\mathcal{K}}_L$ has the following symmetry properties: $\forall \boldsymbol{k} \in \mathbb{R}^3$, $\forall k \in \mathbb{C}$,

$$\boldsymbol{\mathcal{K}}_L(\boldsymbol{k}, -\overline{k}) = \overline{\boldsymbol{\mathcal{K}}_L(\boldsymbol{k}, k)} \tag{28}$$

and

$$\boldsymbol{\mathcal{K}}_L(-\boldsymbol{k}, k) = -\boldsymbol{\mathcal{K}}_L(\boldsymbol{k}, k). \tag{29}$$

Finally, we can make L tend to infinity in Eq. (27), which yields

$$\boldsymbol{\mathcal{K}}(\boldsymbol{k}, k) = \boldsymbol{k} + \imath \, \tfrac{\lambda}{4\pi} \int_{\boldsymbol{s} \in \partial V} \left(\int_{\boldsymbol{u} \in \mathcal{S}(0,1)} \boldsymbol{u} \, \ln \left(\tfrac{\boldsymbol{u}^\top \boldsymbol{\mathcal{K}}(\boldsymbol{k},k) + k \, \widehat{\beta}(\boldsymbol{s},k)}{\boldsymbol{u}^\top \boldsymbol{\mathcal{K}}(\boldsymbol{k},k) - k \, \widehat{\beta}(\boldsymbol{s},k)} \right) d\sigma(\boldsymbol{u} | \boldsymbol{n}(\boldsymbol{s})) \right) dS(\boldsymbol{s}), \tag{30}$$

where the directional measure σ was expressed in Eq. (12). As explained in Remarks 2 and 3, Eq. (30) encompasses both particular cases of mixing billiards and of special polyhedra, since it generalizes the closed-form expressions of the wave vectors distortion in Badeau (2025c, Secs. VI C and VII).

6.3. Black holes

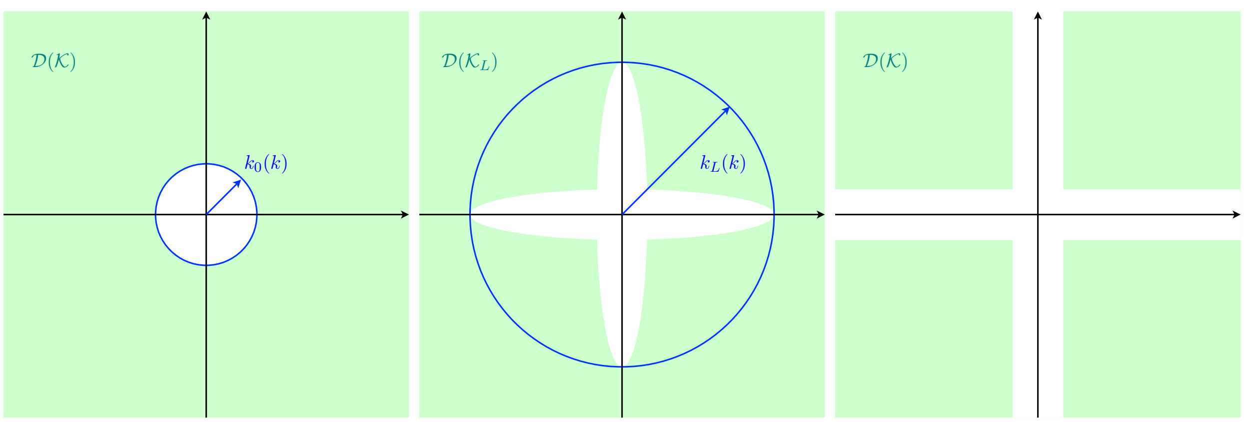

(a) Mixing (isotropic) room (b) Rectangular room, $L < +\infty$ (c) Rectangular room, $L = +\infty$

Figure 1: Domain of the wave vectors distortion function: green represents domain; white represents singularity.

It is shown in Appendix B that, when the series expansion over the basis of real spherical harmonics is truncated to a finite degree $L \in \mathbb{N}$, i.e., when the power and pseudo spectra are locally smoothed in the direction set $\mathcal{S}(0, 1)$, then the domain $\mathcal{D}(\boldsymbol{\mathcal{K}}_L)$ of the wave vectors distortion $\boldsymbol{\mathcal{K}}_L$ introduced in Eq. (27) extends to infinity, which means that its complement $\mathbb{R}^3\backslash\mathcal{D}(\boldsymbol{\mathcal{K}}_L)$ is a bounded subset of $\mathbb{R}^3$. Therefore, the function $\boldsymbol{\mathcal{K}}_L$ is always well-defined at high frequency (i.e., when $f \to +\infty$). In addition, the set $\mathbb{R}^3\backslash\mathcal{D}(\boldsymbol{\mathcal{K}}_L)$ contains singularities of function $\boldsymbol{\mathcal{K}}_L$, in the sense that this function is not well-defined on $\mathbb{R}^3\backslash\mathcal{D}(\boldsymbol{\mathcal{K}}_L)$. At first stance, one might believe that this is because the implicit equation (27) does not admit any solution $\boldsymbol{\mathcal{K}}_L(\boldsymbol{k}, k) \in \mathbb{C}$ when $\boldsymbol{k} \in \mathbb{R}^3\backslash\mathcal{D}(\boldsymbol{\mathcal{K}}_L)$. However, in fact, this is rather the contrary: the function $\boldsymbol{\mathcal{K}}_L$ is not well-defined on $\mathbb{R}^3\backslash\mathcal{D}(\boldsymbol{\mathcal{K}}_L)$ because the implicit equation (27) admits *several* solutions $\boldsymbol{\mathcal{K}}_L(\boldsymbol{k}, k) \in \mathbb{C}$ when $\boldsymbol{k} \in \mathbb{R}^3\backslash\mathcal{D}(\boldsymbol{\mathcal{K}}_L)$ (an example will be provided below).

It can be shown that $\forall L \in \mathbb{N}$, the shape of $\mathcal{D}(\boldsymbol{\mathcal{K}}_L)$ only depends on the geometry of the room, not on the particular value of the specific admittance[2] (different cases are represented in Fig. 1). Moreover, there is a sequence of numbers $\{k_L(k) \geq 0\}_{L\in\mathbb{N}}$ such that $\forall L \in \mathbb{N}$, $\mathbb{R}^3\backslash\mathcal{D}(\boldsymbol{\mathcal{K}}_L) \subset \mathcal{B}(0, k_L(k))$ and reciprocally, $\mathbb{R}^3\backslash\mathcal{B}(0, k_L(k)) \subset \mathcal{D}(\boldsymbol{\mathcal{K}}_L)$. In a mixing (i.e., isotropic) room, all $k_L(k)$ are equal to $k_0(k)$ (the domain $\mathcal{D}(\boldsymbol{\mathcal{K}})$ of the mixing room is illustrated in Fig. 1(a), its boundary is the circle of radius $k_0(k)$). However, in non-isotropic rooms, depending on the room geometry, the sequence of numbers $k_L(k)$ may be increasing and such that $\lim_{L\to+\infty} k_L(k) = +\infty$ (the domain $\mathcal{D}(\boldsymbol{\mathcal{K}}_L)$ of the rectangular room is illustrated in Fig. 1(b) for $L < +\infty$, along with the circle of radius $k_L(k)$, and when $L \to +\infty$, the domain $\mathcal{D}(\boldsymbol{\mathcal{K}})$ is illustrated in Fig. 1(c)). For such geometries, the set $\mathbb{R}^3\backslash\mathcal{D}(\boldsymbol{\mathcal{K}})$, where $\boldsymbol{\mathcal{K}}$ denotes the function introduced in Eq. (30), is unbounded, which means that singularities appear even at high frequency (as illustrated in Fig. 1(c)). This is, e.g., the case of all the special polyhedra that we investigated in Badeau (2025c, Sec. VI).

If in addition $\mathrm{Im}(\widehat{\beta}(\boldsymbol{s}, k)) > 0$, which corresponds to a compliance boundary surface, i.e., a surface with the impedance of a spring as explained in Kuttruff (2014, p. 81), then we showed in Badeau (2025c, Sec. VI) that the singularities in $\mathbb{R}^3\backslash\mathcal{D}(\boldsymbol{\mathcal{K}})$ behave like "black holes", in the sense that the power carried by the wave vectors that "fall" into these black holes stays trapped inside. Be aware that these black holes are different from the *acoustic black holes* in structures (Mironov and Pislyakov, 2002; Pelat *et al.*, 2020), although these two types of black holes share similar properties, as we will show below. In the rest of this section, we investigate the particular case of the rectangular cuboid, in order to better understand the physical properties of the black holes that appear in the general statistical wave field theory.

So, let us consider a rectangular cuboid whose faces are orthogonal to the three axes $l \in \{1, 2, 3\}$ of the Cartesian coordinate system. We assume that the specific admittance is uniform on every face of the cuboid, and for simplicity we further assume that the two parallel faces of the cuboid that are orthogonal to every direction l share the same value $\widehat{\beta}_l(k)$. Then the entries $\mathcal{K}_l(\boldsymbol{k}, k)$ of vector $\boldsymbol{\mathcal{K}}(\boldsymbol{k}, k)$ in Eq. (30) are such that:

$$\mathcal{K}_l(\boldsymbol{k}, k) = k_l + \imath \tfrac{\lambda S_l}{2\pi} \ln\left(\tfrac{\mathcal{K}_l(\boldsymbol{k},k) + k\widehat{\beta}_l(k)}{\mathcal{K}_l(\boldsymbol{k},k) - k\widehat{\beta}_l(k)}\right). \tag{31}$$

If $\widehat{\beta}_l(k) = \imath\widehat{b}_l(k)$ with $\widehat{b}_l(k) > 0$, then in particular $\widehat{\beta}_l(k)$ is purely imaginary, so there is no

[2]The author was able to prove this statement in the specific case of the rectangular cuboid and assumes that it remains valid in the general case.

energy absorption at the two parallel faces of the cuboid that are orthogonal to direction l, and we could expect the wave field to be stationary over space in direction l. However, for $k_l = 0$, Eq. (31) admits two purely imaginary solutions $\mathcal{K}_l(\boldsymbol{k}, k) = \pm\imath x$, where $x \in \mathbb{R}$ is the unique positive solution to the implicit equation

$$x = \frac{\lambda S_l}{2\pi} \ln\left(\frac{x + k\widehat{b}_l(k)}{x - k\widehat{b}_l(k)}\right).$$

When $k\,\widehat{b}_l(k) \to +\infty$, it can be easily shown that x admits the asymptotic expansion

$$x = k\widehat{b}_l(k)\left(1 + 2\exp\left(-\frac{2\pi k\widehat{b}_l(k)}{\lambda S_l}\right)\right).$$

In particular, the two solutions $\mathcal{K}_l(\boldsymbol{k}, k)$ to Eq. (31) are such that

$$\mathcal{K}_l(\boldsymbol{k}, k) \underset{k\widehat{b}_l(k)\to+\infty}{\sim} \pm\imath k\widehat{b}_l(k).$$

That means that the plane waves of the wave vectors $\boldsymbol{\mathcal{K}}(\boldsymbol{k}, k)$ are actually not stationary over space in direction l; on the contrary, their magnitudes vary exponentially as $\exp(\pm 2\pi k\widehat{b}_l(k)x_l)$. Since we assumed that $k\widehat{b}_l(k) \to +\infty$, this implies that the energy of these plane waves is trapped in the neighborhood of the two parallel faces of the cuboid that are orthogonal to direction l. This example illustrates the physical behavior of black holes in the general statistical wave field theory: a part of the energy of the wave field is trapped in the neighborhood of the boundary surface, and is never reflected to the interior of the room. Moreover, such black holes may exist even with the use of nonabsorbing materials only, the absorption being caused by the energy accumulation at the boundary, rather than by the energy transformation to heat, similarly to acoustic black holes in structures (Mironov and Pislyakov, 2002).

6.4. Green's function

From the mathematical developments in Secs. 6.1 and 6.2, the following spectral representation of the Green's function is derived in Appendix C:

$$G(\boldsymbol{x}, \boldsymbol{x}_0, k) = \mu_G(k) + \int_{\boldsymbol{k}\in\mathcal{D}(\boldsymbol{\mathcal{K}}_L)} \int_{\boldsymbol{s}\in\overline{V}} \frac{e^{2\imath\pi\boldsymbol{\mathcal{K}}_L(\boldsymbol{k},k)^\top(\boldsymbol{x}-\boldsymbol{s})}}{4\pi^2(\boldsymbol{\mathcal{K}}_L(\boldsymbol{k},k)^\top\boldsymbol{\mathcal{K}}_L(\boldsymbol{k},k) - k^2)} d\widehat{\xi}_L(\boldsymbol{k}, \boldsymbol{s}), \tag{32}$$

where $\widehat{\xi}_L$ is the same complex random measure as in Eq. (19), and $\mu_G(k)$ was expressed in Eq. (18).

6.5. Source response

Let $\kappa_L(\boldsymbol{k}) \in \mathbb{C}$ be the unique complex solution to the equation

$$\kappa_L(\boldsymbol{k}) = \sqrt{\boldsymbol{\mathcal{K}}_L(\boldsymbol{k}, \kappa_L(\boldsymbol{k}))^\top \boldsymbol{\mathcal{K}}_L(\boldsymbol{k}, \kappa_L(\boldsymbol{k}))} \tag{33}$$

with both non-negative real and imaginary parts[3], and let us define the function

$$\boldsymbol{\kappa}_L(\boldsymbol{k}) = \boldsymbol{\mathcal{K}}_L(\boldsymbol{k}, \kappa_L(\boldsymbol{k})). \tag{34}$$

In Appendix D, based on the spectral representation of the Green's function in Eq. (32), the causal source response p introduced in Eq. (3) is expressed as

$$p(\boldsymbol{x}, \boldsymbol{x}_0, t) = H(t)\, q(\boldsymbol{x}, \boldsymbol{x}_0, t), \tag{35}$$

where the random process q is defined by the following spectral representation:

$$q(\boldsymbol{x}, \boldsymbol{x}_0, t) = c^2\Big(\lambda + \mathrm{Re}\Big(\int_{\boldsymbol{k}\in\mathcal{D}(\boldsymbol{\mathcal{K}}_L)} \int_{\boldsymbol{s}\in\overline{V}} e^{2\imath\pi\left(\boldsymbol{\kappa}_L(\boldsymbol{k})^\top(\boldsymbol{x}-\boldsymbol{s})+c\,\kappa_L(\boldsymbol{k})t\right)} d\widehat{\xi}_L(\boldsymbol{k}, \boldsymbol{s})\Big)\Big). \tag{36}$$

6.6. Simplification of the wave vectors distortion

Substituting Eqs. (27) and (33) into Eq. (34) yields the wave vectors distortion at finite degree L:

$$\boldsymbol{\kappa}_L(\boldsymbol{k}) = \boldsymbol{k} + \imath\,\frac{\lambda}{4\pi}\int_{\boldsymbol{s}\in\partial V}\left(\int_{\boldsymbol{u}\in\mathcal{S}(0,1)} \boldsymbol{u}\,\ln\left(\frac{\boldsymbol{u}^\top\boldsymbol{\kappa}_L(\boldsymbol{k})+\kappa_L(\boldsymbol{k})\,\widehat{\beta}(\boldsymbol{s},\kappa_L(\boldsymbol{k}))}{\boldsymbol{u}^\top\boldsymbol{\kappa}_L(\boldsymbol{k})-\kappa_L(\boldsymbol{k})\,\widehat{\beta}(\boldsymbol{s},\kappa_L(\boldsymbol{k}))}\right)\sigma_L(\boldsymbol{u}, \boldsymbol{n}(\boldsymbol{s}))\, dS(\boldsymbol{u})\right) dS(\boldsymbol{s}), \tag{37}$$

where $\kappa_L(\boldsymbol{k}) \in \mathbb{C}$ is the wave numbers distortion:

$$\kappa_L(\boldsymbol{k}) = \sqrt{\boldsymbol{\kappa}_L(\boldsymbol{k})^\top\boldsymbol{\kappa}_L(\boldsymbol{k})}. \tag{38}$$

When $L \to +\infty$, the density function σ_L tends to the directional measure σ in the sense of Eq. (12). Equations (37)-(38) then yield the asymptotic wave vectors distortion

$$\boldsymbol{\kappa}(\boldsymbol{k}) = \boldsymbol{k} + \imath\,\frac{\lambda}{4\pi}\int_{\boldsymbol{s}\in\partial V}\left(\int_{\boldsymbol{u}\in\mathcal{S}(0,1)} \boldsymbol{u}\,\ln\left(\frac{\boldsymbol{u}^\top\boldsymbol{\kappa}(\boldsymbol{k})+\kappa(\boldsymbol{k})\,\widehat{\beta}(\boldsymbol{s},\kappa(\boldsymbol{k}))}{\boldsymbol{u}^\top\boldsymbol{\kappa}(\boldsymbol{k})-\kappa(\boldsymbol{k})\,\widehat{\beta}(\boldsymbol{s},\kappa(\boldsymbol{k}))}\right) d\sigma(\boldsymbol{u}|\boldsymbol{n}(\boldsymbol{s}))\right) dS(\boldsymbol{s}), \tag{39}$$

where $\kappa(\boldsymbol{k}) \in \mathbb{C}$ denotes the asymptotic wave numbers distortion:

$$\kappa(\boldsymbol{k}) = \sqrt{\boldsymbol{\kappa}(\boldsymbol{k})^\top\boldsymbol{\kappa}(\boldsymbol{k})}. \tag{40}$$

As explained in Sec. 6.3, depending on the room geometry, the set $\mathbb{R}^3\backslash\mathcal{D}(\boldsymbol{\kappa})$ may be unbounded, which means that singularities may appear in the wave vectors distortion of Eq. (39), even at high frequency. In $\mathbb{R}^3\backslash\mathcal{D}(\boldsymbol{\kappa})$, the system of implicit equations (39)-(40) admits several solutions, which may give rise to black holes in the case of a compliance boundary surface (see Sec. 6.3). Computing these solutions requires a numerical solver.

[3]The proof of the existence and uniqueness of the solution with both non-negative real and imaginary parts is a bit lengthy and not essential to our discussion, so we just sketch it quickly here. In the right member of Eq. (33), there exist two square roots of opposite signs. If both are purely imaginary, then their real part is zero and there is one with positive imaginary part, which ends the proof. Otherwise, we can define $\kappa_L(\boldsymbol{k})$ as the one with positive real part. Then proving that its imaginary part is non-negative is equivalent to proving that $\mathrm{Im}(\kappa_L(\boldsymbol{k})^2) \geq 0$. The latter inequality holds asymptotically (when $\|\boldsymbol{k}\| \to +\infty$), and it can be proved by substituting Eq. (27) and the inequalities $\mathrm{Re}(\kappa_L(\boldsymbol{k})) > 0$ and $\mathrm{Re}(\widehat{\beta}) \geq 0$ into Eq. (33).

However, when the series expansion over the basis of real spherical harmonics is truncated to a finite degree L, in the same way as in Sec. 6.3, there is a sequence of numbers $\{k_L \geq 0\}_{L\in\mathbb{N}}$ such that $\forall L \in \mathbb{N}$, $\mathbb{R}^3\backslash\mathcal{D}(\boldsymbol{\kappa}_L) \subset \mathcal{B}(0, k_L)$ and reciprocally, $\mathbb{R}^3\backslash\mathcal{B}(0, k_L) \subset \mathcal{D}(\boldsymbol{\kappa}_L)$. In a mixing (i.e., isotropic) room, all k_L are equal to k_0. However, in non-isotropic rooms, depending on the room geometry, the sequence of numbers k_L may be increasing and such that $\lim_{L\to+\infty} k_L = +\infty$. In all cases, it can be shown as in Appendix B that in $\mathbb{R}^3\backslash\mathcal{B}(0, k_L)$, $\boldsymbol{\kappa}_L(\boldsymbol{k}) - \boldsymbol{k}$ is bounded, and so is $\kappa_L(\boldsymbol{k}) - \|\boldsymbol{k}\|_2$. Thus if $\lim_{k\to+\infty} \frac{d\widehat{\beta}(\boldsymbol{s},k)}{dk} = 0$, then

$$\widehat{\beta}(\boldsymbol{s}, \kappa_L(\boldsymbol{k})) \underset{\|\boldsymbol{k}\|_2\to+\infty}{\sim} \widehat{\beta}(\boldsymbol{s}, \|\boldsymbol{k}\|_2).$$

Therefore, when $\boldsymbol{k} \to +\infty$, the set of implicit equations (37)-(38) is asymptotically equivalent to the following set of explicit equations:

$$\boldsymbol{\kappa}_L(\boldsymbol{k}) = \boldsymbol{k} + \imath \tfrac{\lambda}{4\pi} \int_{\boldsymbol{s}\in\partial V} \int_{\boldsymbol{u}\in\mathcal{S}(0,1)} \boldsymbol{u} \ln\left(\tfrac{\boldsymbol{u}^\top\boldsymbol{k}+\|\boldsymbol{k}\|_2\,\widehat{\beta}(\boldsymbol{s},\|\boldsymbol{k}\|_2)}{\boldsymbol{u}^\top\boldsymbol{k}-\|\boldsymbol{k}\|_2\,\widehat{\beta}(\boldsymbol{s},\|\boldsymbol{k}\|_2)}\right) \sigma_L(\boldsymbol{u}, \boldsymbol{n}(\boldsymbol{s}))\, dS(\boldsymbol{u}) dS(\boldsymbol{s}), \tag{41}$$

and

$$\kappa_L(\boldsymbol{k}) = \|\boldsymbol{k}\|_2 + \imath \tfrac{\lambda}{4\pi} \int_{\boldsymbol{s}\in\partial V} \int_{\boldsymbol{u}\in\mathcal{S}(0,1)} \tfrac{\boldsymbol{u}^\top\boldsymbol{k}}{\|\boldsymbol{k}\|_2} \ln\left(\tfrac{\boldsymbol{u}^\top\boldsymbol{k}+\|\boldsymbol{k}\|_2\widehat{\beta}(\boldsymbol{s},\|\boldsymbol{k}\|_2)}{\boldsymbol{u}^\top\boldsymbol{k}-\|\boldsymbol{k}\|_2\widehat{\beta}(\boldsymbol{s},\|\boldsymbol{k}\|_2)}\right) \sigma_L(\boldsymbol{u}, \boldsymbol{n}(\boldsymbol{s})) dS(\boldsymbol{u}) dS(\boldsymbol{s}). \tag{42}$$

With this new system of equations, there is no need for a numerical solver. However, the reader should keep in mind that the approximation involved in equations (41)-(42) eliminates any possible singularity by enforcing angular smoothing in the wave vector space. In particular, it cannot account for black holes. Moreover, this approximation holds only at frequencies $f > ck_L$, where, depending on the room geometry, the sequence k_L may tend to infinity when $L \to +\infty$. For such geometries, the higher L, the lower the angular smoothing in the wave vector space, and the higher $\|\boldsymbol{k}\|$ must be for equations (41)-(42) to hold.

6.7. *Wigner distribution*

The asymptotic expansion of the cross-Wigner distribution of the random process q, which holds when $f \to +\infty$, is derived in Appendix E from the spectral representation in Eq. (36):

$$W_q(\boldsymbol{x}_1, \boldsymbol{x}_2, \boldsymbol{x}_0, f, t) = \tfrac{c^3}{4} \int_{\boldsymbol{k}\in\mathcal{S}(0,\frac{f}{c})} e^{-2\alpha_L(\boldsymbol{k})t + 2\imath\pi\boldsymbol{k}^\top(\boldsymbol{x}_1-\boldsymbol{x}_2)} \widehat{\Gamma}_{\boldsymbol{\kappa}_L}(\tfrac{\boldsymbol{x}_1+\boldsymbol{x}_2}{2}, \boldsymbol{k})\, dS(\boldsymbol{k}), \tag{43}$$

where $\alpha_L(\boldsymbol{k})$ is the anisotropic temporal attenuation:

$$\begin{aligned} \alpha_L(\boldsymbol{k}) &\triangleq 2\pi c\, \mathrm{Im}(\kappa_L(\boldsymbol{k})) \\ &= \tfrac{\lambda c}{4} \int_{\boldsymbol{s}\in\partial V} \left(\int_{\boldsymbol{u}\in\mathcal{S}(0,1)} \tfrac{\boldsymbol{u}^\top\boldsymbol{k}}{\|\boldsymbol{k}\|_2} \ln\left(\left|\tfrac{\boldsymbol{u}^\top\boldsymbol{k}+\|\boldsymbol{k}\|_2\,\widehat{\beta}(\boldsymbol{s},\|\boldsymbol{k}\|_2)}{\boldsymbol{u}^\top\boldsymbol{k}-\|\boldsymbol{k}\|_2\,\widehat{\beta}(\boldsymbol{s},\|\boldsymbol{k}\|_2)}\right|^2\right) \sigma_L(\boldsymbol{u}, \boldsymbol{n}(\boldsymbol{s}))\, dS(\boldsymbol{u})\right) dS(\boldsymbol{s}), \end{aligned} \tag{44}$$

which is obtained from Eq. (42). In Eq. (43), the distorted power spectrum $\widehat{\Gamma}_{\boldsymbol{\kappa}_L}(\boldsymbol{x}, \boldsymbol{k})$ is a smooth function of both $\boldsymbol{x}$ and $\boldsymbol{k}$:

$$\widehat{\Gamma}_{\boldsymbol{\kappa}_L}(\boldsymbol{x}, \boldsymbol{k}) = \int_{\boldsymbol{s}\in\overline{V}} e^{-4\pi\mathrm{Im}(\boldsymbol{\kappa}_L(\boldsymbol{k}))^\top(\boldsymbol{x}-\boldsymbol{s})} \frac{d\widehat{\Lambda}_L^0\left((\mathrm{Re}\,\boldsymbol{\kappa}_L)^{-1}(\boldsymbol{k}), \boldsymbol{s}\right)}{\left|\det\left(\mathrm{Jac}_{\mathrm{Re}\,\boldsymbol{\kappa}_L}\left((\mathrm{Re}\,\boldsymbol{\kappa}_L)^{-1}(\boldsymbol{k})\right)\right)\right|}, \tag{45}$$

where function $\boldsymbol{\kappa}_L(\boldsymbol{k})$ was expressed in Eq. (41), and $\widehat{\Lambda}^0_L(\boldsymbol{k}, \mathcal{V})$ denotes the smooth density w.r.t. $\boldsymbol{k}$ of the spectral measure $\widehat{\Lambda}_L(\mathcal{K}, \mathcal{V})$ defined in Eq. (21):

$$\widehat{\Lambda}^0_L(\boldsymbol{k}, \mathcal{V}) = \lambda^2 \Big(|\mathcal{V}| + \tfrac{1}{4} \int_{\boldsymbol{s} \in \mathcal{V} \cap \partial V} \int_{\boldsymbol{u} \in \mathcal{S}(0,1)} \delta\left(\boldsymbol{u}^\top \boldsymbol{k}\right)\, \sigma_L(\boldsymbol{u}, \boldsymbol{n}(\boldsymbol{s}))\, dS(\boldsymbol{u})\, dS(\boldsymbol{s}) \Big), \tag{46}$$

which is such that

$$\widehat{\Lambda}_L(\mathcal{K}, \mathcal{V}) = \int_{\boldsymbol{k} \in \mathcal{K}} \int_{\boldsymbol{s} \in \mathcal{V}} d\widehat{\Lambda}^0_L(\boldsymbol{k}, \boldsymbol{s}) d\boldsymbol{k}.$$

Note that, when $\widehat{\beta} = 0$, the closed-form expression of the distorted power spectrum $\widehat{\Gamma}_{\boldsymbol{\kappa}_L}(\boldsymbol{x}, \boldsymbol{k})$ in Eq. (45) reduces to that of the power spectrum $\widehat{\Gamma}_L(\boldsymbol{k})$ in Eq. (22), which was derived in the case of Neumann's boundary condition.

If in addition we assume that $\frac{d\widehat{\beta}(\boldsymbol{s},k)}{dk} = o(\frac{1}{k})$, then Eq. (45) yields the following first order expansion:

$$\begin{aligned} &\widehat{\Gamma}_{\boldsymbol{\kappa}_L}(\boldsymbol{x}, \boldsymbol{k}) \\ &= \lambda^2 \Bigg(\left(1 + \frac{\lambda \int_{\boldsymbol{s} \in \partial V} \int_{\boldsymbol{u} \in \mathcal{S}(0,1)} \left(\frac{(\boldsymbol{u}^\top \boldsymbol{k})^2 - \|\boldsymbol{k}\|_2^2}{2\pi} \mathrm{Im}\left(\frac{\widehat{\beta}(\boldsymbol{s}, \|\boldsymbol{k}\|_2)}{(\boldsymbol{u}^\top \boldsymbol{k})^2 - \|\boldsymbol{k}\|_2^2 \widehat{\beta}(\boldsymbol{s}, \|\boldsymbol{k}\|_2)^2} \right) + \frac{\mathrm{sign}(\mathrm{Im}(\widehat{\beta}(\boldsymbol{s}, \|\boldsymbol{k}\|_2)) \delta\left(\frac{\boldsymbol{u}^\top \boldsymbol{k}}{\|\boldsymbol{k}\|_2} \right)}{2} \right) \sigma_L(\boldsymbol{u}, \boldsymbol{n}(\boldsymbol{s})) dS(\boldsymbol{u}) dS(\boldsymbol{s})}{\|\boldsymbol{k}\|_2} \right) \\ &\times \int_{\boldsymbol{s} \in V} e^{-4\pi \mathrm{Im}(\boldsymbol{\kappa}_L(\boldsymbol{k}))^\top (\boldsymbol{x} - \boldsymbol{s})} d\boldsymbol{s} + \frac{\int_{\boldsymbol{s} \in \partial V} e^{-4\pi \mathrm{Im}(\boldsymbol{\kappa}_L(\boldsymbol{k}))^\top (\boldsymbol{x} - \boldsymbol{s})} \int_{\boldsymbol{u} \in \mathcal{S}(0,1)} \delta\left(\frac{\boldsymbol{u}^\top \boldsymbol{k}}{\|\boldsymbol{k}\|_2} \right) \sigma_L(\boldsymbol{u}, \boldsymbol{n}(\boldsymbol{s}))\, dS(\boldsymbol{u})\, dS(\boldsymbol{s})}{4 \|\boldsymbol{k}\|_2} \Bigg). \end{aligned} \tag{47}$$

Finally, when $\boldsymbol{x}_1 = \boldsymbol{x}_2 = \boldsymbol{x}$, Eq. (43) yields the expression of the power distribution jointly over space, frequency and time:

$$W_q(\boldsymbol{x}, \boldsymbol{x}, \boldsymbol{x}_0, f, t) = \tfrac{c^3}{4} \int_{\boldsymbol{k} \in \mathcal{S}(0, \frac{f}{c})} e^{-2\alpha_L(\boldsymbol{k}) t}\, \widehat{\Gamma}_{\boldsymbol{\kappa}_L}(\boldsymbol{x}, \boldsymbol{k})\, dS(\boldsymbol{k}). \tag{48}$$

In the case of mixing billiards that we addressed in Badeau (2024, Sec. VI F), we showed that the cross-Wigner distribution was factorizable as the product of a function of space and a function of time at fixed frequency f, as in Polack's formula (Polack, 1988). So in mixing rooms, the power distribution at any frequency f decreases exponentially over time. However, in the anisotropic case, the cross-Wigner distribution $W_q(\boldsymbol{x}_1, \boldsymbol{x}_2, \boldsymbol{x}_0, f, t)$ in Eq. (43) can no longer be factorized in the same way. So it is no longer an exponential function of time. In particular, the temporal profile of the power distribution $W_q(\boldsymbol{x}, \boldsymbol{x}, \boldsymbol{x}_0, f, t)$ in Eq. (48) at any frequency f is rather a linear combination of infinitely many decreasing exponentials. We thus retrieve a well-known result in room acoustics: the time decay in non-ergodic rooms is not exponential [see, e.g., (Kanev, 2012; Kuttruff, 2014)]. Nevertheless, Eq. (44) permits us to establish an important result that was unknown so far: the closed-form expression of the directional reverberation time in semi-ergodic rooms:

$$T_{60}(\boldsymbol{k}) \triangleq \frac{3 \ln(10)}{\alpha_L(\boldsymbol{k})} = \frac{24 \ln(10)}{c} \frac{|V|}{-2 \int_{\boldsymbol{s} \in \partial V} \left(\int_{\boldsymbol{u} \in \mathcal{S}(0,1)} \ln\left(1 - a\left(\boldsymbol{s}, \|\boldsymbol{k}\|_2, \frac{|\boldsymbol{u}^\top \boldsymbol{k}|}{\|\boldsymbol{k}\|_2}\right)\right) \frac{|\boldsymbol{u}^\top \boldsymbol{k}|}{\|\boldsymbol{k}\|_2} \sigma_L(\boldsymbol{u}, \boldsymbol{n}(\boldsymbol{s}))\, dS(\boldsymbol{u}) \right) dS(\boldsymbol{s})}, \tag{49}$$

where $a(\boldsymbol{s}, k, \gamma) = 1 - \left| \frac{\gamma - \widehat{\beta}(\boldsymbol{s},k)}{\gamma + \widehat{\beta}(\boldsymbol{s},k)} \right|^2$. Physically, Eq. (49) can be interpreted as follows: for a plane wave of wave vector $\boldsymbol{k}$ and for any point $\boldsymbol{s} \in \partial V$ on the boundary surface,

- the outward normal $\boldsymbol{n}(\boldsymbol{s})$ of the boundary surface at $\boldsymbol{s}$ is seen, through the successive reflections of the plane wave over the boundary surface, as a random vector $\boldsymbol{u} \in \mathcal{S}(0,1)$, of probability density function $\sigma_L(\boldsymbol{u}, \boldsymbol{n}(\boldsymbol{s}))$ over the unit sphere $\mathcal{S}(0,1)$ (see Remark 1);
- the angle of incidence θ of the plane wave on the boundary surface at $\boldsymbol{s}$ is such that $\cos(\theta) = \frac{\boldsymbol{u}^\top \boldsymbol{k}}{\|\boldsymbol{k}\|_2}$;
- $|\cos(\theta)| dS(\boldsymbol{s})$ is the apparent area of the surface element $dS(\boldsymbol{s})$ for the plane wave;
- $a(\boldsymbol{s}, \|\boldsymbol{k}\|_2, |\cos(\theta)|) \in [0,1]$ is the absorption coefficient of the boundary surface at point $\boldsymbol{s}$, frequency $f = c\|\boldsymbol{k}\|_2$, and angle θ.

Note that Eq. (49) can be rewritten in the same form as Eyring's formula (Eyring, 1930) as expressed in Badeau (2024, Sec. III F 2), except that in the case of anisotropic wave fields, $T_{60}(\boldsymbol{k})$ depends not only on the norm of wave vector $\boldsymbol{k}$, but also on its direction:

$$T_{60}(\boldsymbol{k}) = \frac{24\ln(10)}{c} \frac{|V|}{-\int_{\boldsymbol{s}\in\partial V} \ln(1-a(\boldsymbol{s},\boldsymbol{k}))dS(\boldsymbol{s})}, \tag{50}$$

where the average directional absorption coefficient $a(\boldsymbol{s}, \boldsymbol{k})$ is defined as

$$a(\boldsymbol{s}, \boldsymbol{k}) = 1 - e^{2\int_{\boldsymbol{u}\in\mathcal{S}(0,1)} \ln\left(1-a\left(\boldsymbol{s}, \|\boldsymbol{k}\|_2, \frac{|\boldsymbol{u}^\top\boldsymbol{k}|}{\|\boldsymbol{k}\|_2}\right)\right) \frac{|\boldsymbol{u}^\top\boldsymbol{k}|}{\|\boldsymbol{k}\|_2} \sigma_L(\boldsymbol{u},\boldsymbol{n}(\boldsymbol{s}))\, dS(\boldsymbol{u})}, \tag{51}$$

which involves a geometric mean over all angles of incidence. In the isotropic case, $\sigma_L(\boldsymbol{u}, \boldsymbol{v}) = \frac{1}{4\pi}$ as shown in Eq. (14), then $T_{60}(\boldsymbol{k})$ and $a(\boldsymbol{s}, \boldsymbol{k})$ depend only on $k = \|\boldsymbol{k}\|_2$, and Eq. (50) reduces exactly to the Eyring-like formula presented in Badeau (2024, Eq. (41)). Moreover, Eq. (51) reduces to Badeau (2024, Eqs. (125)-(126)).

In other respects, in the general anisotropic case, when the average directional absorption coefficient $a(\boldsymbol{s}, \boldsymbol{k})$ is small, Eqs. (50) and (51) yield

$$T_{60}(\boldsymbol{k}) = \frac{24\ln(10)}{c} \frac{|V|}{\int_{\boldsymbol{s}\in\partial V} a(\boldsymbol{s},\boldsymbol{k})dS(\boldsymbol{s})} \tag{52}$$

and

$$a(\boldsymbol{s}, \boldsymbol{k}) = 2\int_{\boldsymbol{u}\in\mathcal{S}(0,1)} a\left(\boldsymbol{s}, \|\boldsymbol{k}\|_2, \frac{|\boldsymbol{u}^\top\boldsymbol{k}|}{\|\boldsymbol{k}\|_2}\right) \frac{|\boldsymbol{u}^\top\boldsymbol{k}|}{\|\boldsymbol{k}\|_2} \sigma_L(\boldsymbol{u}, \boldsymbol{n}(\boldsymbol{s}))\, dS(\boldsymbol{u}), \tag{53}$$

which now involve an arithmetic mean over all angles of incidence. Then, again in the particular isotropic case, $T_{60}(\boldsymbol{k})$ and $a(\boldsymbol{s}, \boldsymbol{k})$ depend only on $k = \|\boldsymbol{k}\|_2$, and Eq. (52) reduces exactly to Sabine's formula (Badeau, 2024, Eq. (40)). Moreover, Eq. (53) can be rewritten in the form $a(\boldsymbol{s}, k) = \int_{\theta=0}^{\frac{\pi}{2}} a(\boldsymbol{s}, k, \cos(\theta)) \sin(2\theta)\, d\theta$, which is exactly the *Paris* formula of the average absorption coefficient for a random, uniformly and isotropically distributed sound incidence, as expressed in Kuttruff (2014, p. 55) and Morse and Ingard (1968, p. 580). We can thus conclude that Eq. (51) is both more accurate and more general than the Paris formula, because it also holds at higher absorption and in anisotropic rooms.

In the particular case of the rectangular cuboid, Eq. (49) is very close to Bilbao and Alary (2024, Eq. (34)). Actually, Eq. (49) would exactly reduce to Bilbao and Alary (2024, Eq. (34)) if the probability measure $\sigma_L(\boldsymbol{u}, \boldsymbol{n}(\boldsymbol{s}))dS(\boldsymbol{u})$ were replaced by its limit $d\sigma(\boldsymbol{u}, \boldsymbol{n}(\boldsymbol{s}))$ when $L \to \infty$. However, doing so would be inconsistent because the singularities in the wave vector space would be eliminated without applying angular smoothing. We can thus conclude that Bilbao and Alary (2024, Eq. (34)) is almost accurate, except that it does not account for the existence of black holes in the rectangular cuboid. This is due to the approach used by the authors, based on the image source method, which only provides an approximation of the wave field in the case of Robin's boundary condition.

Finally, as already discussed in Sec. 4.1, it may be more convenient in applications to consider the cross-Wigner distribution of the RIR $h(\boldsymbol{x}, \boldsymbol{x}_0, t)$ rather than that of the random process $q(\boldsymbol{x}, \boldsymbol{x}_0, t)$. By substituting Eq. (17) into Eq. (43), we thus get the asymptotic expansion of $W_h(\boldsymbol{x}_1, \boldsymbol{x}_2, \boldsymbol{x}_0, f, t)$, which holds when $f \to +\infty$:

$$W_h(\boldsymbol{x}_1, \boldsymbol{x}_2, \boldsymbol{x}_0, f, t) = \frac{c^3}{4} \int_{\boldsymbol{k} \in \mathcal{S}(0, \frac{f}{c})} \frac{e^{-2\alpha_L(\boldsymbol{k})t + 2\imath\pi \boldsymbol{k}^\top (\boldsymbol{x}_1 - \boldsymbol{x}_2)}}{4\pi^2 f^2 + \alpha_L(\boldsymbol{k})^2} \, \widehat{\Gamma}_{\boldsymbol{\kappa}_L}\left(\tfrac{\boldsymbol{x}_1 + \boldsymbol{x}_2}{2}, \boldsymbol{k}\right) dS(\boldsymbol{k}).$$

7. Conclusion

In this paper, we extended the statistical wave field theory presented in Badeau (2024) to the class of semi-mixing billiards introduced in Badeau (2026), in the general case of Robin's boundary condition. We have shown that when there is energy absorption at the boundary, contrary to the mixing case, at fixed frequency in these semi-mixing billiards, the power distribution is no longer an exponential function of time: the temporal profile of the power distribution is rather a linear combination of infinitely many decreasing exponentials. We thus retrieved a well-known fact in room acoustics: the time decay in non-ergodic rooms is not exponential (Kanev, 2012; Kuttruff, 2014). However, we were able to show that such anisotropic wave fields are characterized by a directional reverberation time that is independent of the receiver's position but depends on its orientation, and we have provided its closed-form expression [Eq. (49)], which improves and generalizes both Eyring's formula of the reverberation time in ergodic rooms (Eyring, 1930), and Bilbao and Alary's formula of the directional reverberation time in the shoebox room (Bilbao and Alary, 2024). We showed that this general formula of the directional reverberation time could be interpreted by means of simple physical arguments involving the statistics of the successive reflections of plane waves over the boundary surface, which are directly related to the statistics of the ray trajectories in the underlying classical billiard. Nevertheless, we believe that deriving this formula directly from such simple physical considerations, without the help of the statistical wave field theory, would have been hardly feasible. Finally, this study of directional reverberation resulted in the definition a directional absorption coefficient of the surfaces, which is explicitly related to the specific admittance of Robin's boundary condition.

Regarding the experimental verification of the theory presented in this paper, the prediction of the isotropic reverberation time in mixing rooms, which is a particular case of Eq. (49), has already been proved accurate in Prinn and Badeau (2026), where it was compared to various numerical models. In addition, the prediction of the directional reverberation time in anisotropic rooms by Eq. (49) is accurate in the case of special polyhedra, because in this case the wave vectors distortion in Eq. (30) matches exactly the existing closed-form expressions of the eigenfunctions (Badeau, 2025c). Moreover, in the particular case of the rectangular cuboid, Eq. (49) reduces to Bilbao and Alary (2024, Eq. (34)), which was derived in a completely different way. Finally, in order to further validate Eq. (49), it would be possible to perform numerical simulations of anisotropic rooms that are not integrable, such as any rational polyhedron that is not one of the special polyhedra.

In summary, the contributions of the statistical wave field theory to the field of room acoustics are numerous:

- it provides a *unified framework* that encompasses all the previously known statistical properties of late reverberation, including the reverberation time (Sec. 6.7);
- it provides a *global description* of the wave field, through the closed-form expression of its power distribution and correlations over time, frequency and space (Sec. 6.7 and (Badeau, 2026, Sec. V D));
- it is applicable to a *large class of room shapes*: the anisotropic version of the theory presented in this paper goes beyond the original class of mixing billiards (Secs. 1 and 3);
- it is *more accurate* than the existing approaches based on the statistics of reflections in classical billiards, thanks to the semiclassical approximation of quantum physics (Secs. 1 and 4.2);
- it reveals the existence of *black holes*, which behave like those of general relativity: a part of the energy is trapped in the vicinity of the domain's boundary (Sec. 6.3).

In future work, an obvious application of the anisotropic version of the statistical wave field theory is the analysis and synthesis of directional reverberation, which seems to be a topical issue, considering the many related references that we mentioned in the introduction, including a recent PhD thesis (Alary, 2021). In other respects, the formulas of the directional reverberation time presented in Sec. 6.7 pave the way for a possible estimation of the physical parameters (directional absorption, admittance) of various materials from late reverberation measurements.

The theoretical work presented in this paper could also be extended in various ways. For instance, as we already showed in Badeau (2025b), pursuing the asymptotic expansion of the (pseudo) spectral measure, and thus of the wave vectors distortion, beyond the first order term, is of much interest because it allows the theory predictions to hold at lower frequencies. So far, we have already investigated in Badeau (2025b) the isotropic second-order *curvature term* in mixing billiards, which accounts for the impact of a curved boundary surface on the wave field statistics, under both Neumann and Robin's boundary conditions. This work could be generalized to the class of semi-mixing billiards that we considered here. In other respects, we also have investigated the anisotropic second-order *edge term*, which accounts for edge diffusion, in Badeau (2025c), in the particular case of special polyhedra and under Neumann's boundary condition. This work could be generalized to the class of semi-mixing billiards, and also to Robin's boundary condition.

Acknowledgments

The author would like to thank the anonymous reviewers for their very helpful comments, which greatly contributed to making this article more accessible.

Author Declarations

Conflict of Interest: The author of this paper has no conflict of interest to disclose.

Data Availability

Data sharing is not applicable to this article as no new data were created or analyzed in this study.

Appendix A.

In this appendix, we derive the closed-form expression of the anisotropic pseudo spectrum $\widehat{J}_L$, which was given in Eq. (24). As in Badeau (2024, Sec. VI A), we start by considering a local version $\widehat{\mathcal{J}}_L(\mathcal{K}, \mathcal{V}, k)$ of the pseudo spectral measure $\widehat{J}_B(\mathcal{K}, k)$ introduced in Sec. 4.2, first in a vicinity $\mathcal{V} \subset V$ of any interior point $\boldsymbol{s} \in V$ (Sec. Appendix A.1), then in a vicinity $\mathcal{V} \subset \overline{V}$ of any boundary point $\boldsymbol{s} \in \partial V$ (Sec. Appendix A.2), before introducing the consolidated expression of the pseudo spectral measure $\widehat{\mathcal{J}}_L(\mathcal{K}, \mathcal{V}, k)$ that holds in any region $\mathcal{V} \subseteq \overline{V}$ (Sec. Appendix A.3). The closed-form expression of $\widehat{J}_L$ is finally obtained for $\mathcal{V} = \overline{V}$.

Appendix A.1. Interior points

In a vicinity $\mathcal{V} \subset V$ of a point $\boldsymbol{s} \in V$, by using the mathematical developments in Badeau (2024, Sec. VI A 1), we get $\widehat{\mathcal{J}}(\boldsymbol{\kappa}, \mathcal{V}, k) = \lambda^2 |\mathcal{V}|$, hence the following expression of the pseudo spectral measure:

$$\widehat{\mathcal{J}}_L(\mathcal{K}, \mathcal{V}, k) = \lambda^2 |\mathcal{K}||\mathcal{V}|. \tag{A.1}$$

In Appendix A.2, the directional measure σ expressed in Eq. (12) will be replaced by its truncation to a finite degree L defined in Eq. (13). The notation $\widehat{\mathcal{J}}_L$ instead of $\widehat{\mathcal{J}}$ in Eq. (A.1) reflects this dependence on the degree L. Note that this pseudo spectral measure $\widehat{\mathcal{J}}_L$ is innately isotropic (it corresponds to free field propagation), so that its expression is not affected by the successive reflections over the billiard's boundary.

Appendix A.2. Boundary points

As done in Balian and Bloch (1970, Sec. III-A), we now use the *plane approximation*: the boundary surface in the vicinity $\mathcal{V}$ of a point $\boldsymbol{s} \in \partial V$, i.e., $\mathcal{V} \cap \partial V$, is approximated by $\mathcal{V} \cap T(\boldsymbol{s})$, where $T(\boldsymbol{s})$ is the plane tangent to ∂V at $\boldsymbol{s}$. This approximation is justified at high frequency (second assumption in Sec. 4.2). By using the mathematical developments in Badeau (2024, Sec. VI A 2), we get

$$\widehat{\mathcal{J}}(\boldsymbol{\kappa}, \mathcal{V}, k) = \lambda^2 \Big(|\mathcal{V}| + \tfrac{S(\mathcal{V} \cap T(\boldsymbol{s}))}{4\pi} \Big(\tfrac{1}{\imath \boldsymbol{n}(\boldsymbol{s})^\top \boldsymbol{\kappa}} - \pi \delta(\boldsymbol{n}(\boldsymbol{s})^\top \boldsymbol{\kappa}) + \tfrac{2\imath}{\boldsymbol{n}(\boldsymbol{s})^\top \boldsymbol{\kappa} - k \widehat{\beta}(\boldsymbol{s}, k)} \Big) \Big). \tag{A.2}$$

Then, by proceeding exactly in the same way as we did in Badeau (2026, Subsection 2 of Appendix B), we get from Eq. (A.2) the closed-form expression of the pseudo spectral measure $\widehat{\mathcal{J}}_L$ on $\mathbb{R}^3 \times \overline{V}$:

$$\begin{aligned} \widehat{\mathcal{J}}_L(\mathcal{K}, \mathcal{V}, k) = \quad & \lambda^2 \Big(|\mathcal{K}||\mathcal{V}| + \tfrac{S(\mathcal{V} \cap T(\boldsymbol{s}))}{4\pi} \int_{\boldsymbol{\kappa} \in \mathcal{K}} \int_{\boldsymbol{u} \in \mathcal{S}(0,1)} \\ & \Big(-\pi \delta\left(\boldsymbol{u}^\top \boldsymbol{\kappa}\right) - \tfrac{\imath}{\boldsymbol{u}^\top \boldsymbol{\kappa} + k \widehat{\beta}(\boldsymbol{s}, k)} + \tfrac{\imath}{\boldsymbol{u}^\top \boldsymbol{\kappa} - k \widehat{\beta}(\boldsymbol{s}, k)} \Big) \sigma_L(\boldsymbol{u}, \boldsymbol{n}(\boldsymbol{s})) \, dS(\boldsymbol{u}) \, d\boldsymbol{\kappa} \Big). \end{aligned} \tag{A.3}$$

Note that this equation follows from the expression of the B-function in a half-space delimited by a plane boundary [Eq. (29) in Badeau (2024)], which holds only when $\mathrm{Im}(k\,\widehat{\beta}(\boldsymbol{s},k)) < 0$, therefore Eq. (A.3) also holds only when $\mathrm{Im}(k\,\widehat{\beta}(\boldsymbol{s},k)) < 0$. In Badeau (2024, Sec. VI C), in the particular case of mixing billiards, the analyticity of the Green's function $G(\boldsymbol{x},\boldsymbol{x}_0,k)$ permitted us to get the closed-form expression of its spectral representation that holds $\forall\widehat{\beta}(\boldsymbol{s},k) \in \mathbb{C}$, without needing to calculate $\widehat{\mathcal{J}}_L(\mathcal{K},\mathcal{V},k)$ for $\mathrm{Im}(k\,\widehat{\beta}(\boldsymbol{s},k)) > 0$. Here however, in order to investigate the general case of anisotropic wave fields in every detail, we provide the expression of $\widehat{\mathcal{J}}_L(\mathcal{K},\mathcal{V},k)$ that holds in all cases.

First, let us define the function

$$\psi(x,z) = \ln\left(\frac{x+z}{x-z}\right) \tag{A.4}$$

for $x \in \mathbb{R}$ and $z \in \mathbb{C} - \mathbb{R}$. Then, note that when $x \to 0$,

$$\frac{x+z}{x-z} = -\left(1 + \frac{2\mathrm{Re}(z)}{|z|^2}x\right) + \imath\frac{2\mathrm{Im}(z)}{|z|^2}x + O(x^2).$$

Because of the discontinuity of the principal branch of the complex logarithm on $\mathbb{R}_-$, we deduce that $\lim_{x\to 0^+}\psi(x,z) = +\imath\pi\,\mathrm{sign}(\mathrm{Im}(z))$, whereas $\lim_{x\to 0^-}\psi(x,z) = -\imath\pi\,\mathrm{sign}(\mathrm{Im}(z))$. Therefore, the derivative of function ψ w.r.t. x in the sense of distributions is

$$\psi'(x,z) = \frac{1}{x+z} - \frac{1}{x-z} + \imath 2\pi\,\mathrm{sign}(\mathrm{Im}(z))\,\delta(x). \tag{A.5}$$

In particular, we note that when $z \to 0$, $\psi(x,z) \to 0$ $\forall x \in \mathbb{R}\backslash\{0\}$, therefore $\psi'(x,z) \to 0$ in the sense of distributions. Based on this remark, Eq. (A.3), which holds when $\mathrm{Im}(k\,\widehat{\beta}(\boldsymbol{s},k)) < 0$, can be rewritten in the following form:

$$\begin{aligned}\widehat{\mathcal{J}}_L(\mathcal{K},\mathcal{V},k) = \;& \lambda^2\Big(|\mathcal{K}||\mathcal{V}| + \tfrac{S(\mathcal{V}\cap T(\boldsymbol{s}))}{4\pi}\int_{\boldsymbol{\kappa}\in\mathcal{K}}\int_{\boldsymbol{u}\in\mathcal{S}(0,1)} \\ & \Big(\pi\left(1+2\,\mathrm{sign}(\mathrm{Im}(k\,\widehat{\beta}(\boldsymbol{s},k)))\right)\delta\left(\boldsymbol{u}^\top\boldsymbol{\kappa}\right) - \tfrac{\imath}{\boldsymbol{u}^\top\boldsymbol{\kappa}+k\widehat{\beta}(\boldsymbol{s},k)} + \tfrac{\imath}{\boldsymbol{u}^\top\boldsymbol{\kappa}-k\widehat{\beta}(\boldsymbol{s},k)}\Big) \\ & \times\sigma_L(\boldsymbol{u},\boldsymbol{n}(\boldsymbol{s}))\,dS(\boldsymbol{u})\,d\boldsymbol{\kappa}\Big).\end{aligned} \tag{A.6}$$

Indeed, when $\widehat{\beta}(\boldsymbol{s},k) \to 0$, Eq. (A.6) shows that $\widehat{\mathcal{J}}_L(\mathcal{K},\mathcal{V},k)$ converges as expected to the spectral measure $\widehat{\Lambda}_L(\mathcal{K},\mathcal{V})$ in Badeau (2026, Eq. (B6)), which was established in the case of Neumann's boundary condition. By continuation of the analytic terms in Eq. (A.6), and because $\widehat{\mathcal{J}}_L(\mathcal{K},\mathcal{V},k)$ must also converge to $\widehat{\Lambda}_L(\mathcal{K},\mathcal{V})$ when $\mathrm{Im}(k\,\widehat{\beta}(\boldsymbol{s},k)) > 0$, we conclude that Eq. (A.6) is actually the correct expression of the pseudo spectral measure $\widehat{\mathcal{J}}_L(\mathcal{K},\mathcal{V},k)$ that holds $\forall\widehat{\beta}(\boldsymbol{s},k) \in \mathbb{C}$.

Appendix A.3. Consolidated pseudo spectral measure

In the same way as we did in Badeau (2024, Sec. VI A 3), by integrating over all points $\boldsymbol{s} \in \overline{V}$, we get from Eqs. (A.1) and (A.6) the consolidated expression of the pseudo spectral measure on $\mathbb{R}^3 \times \overline{V}$:

$$\begin{aligned}\widehat{\mathcal{J}}_L(\mathcal{K},\mathcal{V},k) = \ & \lambda^2\Big(|\mathcal{K}||\mathcal{V}| + \tfrac{1}{4\pi}\int_{\boldsymbol{\kappa}\in\mathcal{K}}\int_{\boldsymbol{s}\in\mathcal{V}\cap\partial V}\int_{\boldsymbol{u}\in\mathcal{S}(0,1)} \\ & \Big(\pi\left(1+2\,\mathrm{sign}(\mathrm{Im}(k\,\widehat{\beta}(\boldsymbol{s},k)))\right)\delta\left(\boldsymbol{u}^\top\boldsymbol{\kappa}\right) - \tfrac{\imath}{\boldsymbol{u}^\top\boldsymbol{\kappa}+k\widehat{\beta}(\boldsymbol{s},k)} + \tfrac{\imath}{\boldsymbol{u}^\top\boldsymbol{\kappa}-k\widehat{\beta}(\boldsymbol{s},k)}\Big) \\ & \times\sigma_L(\boldsymbol{u},\boldsymbol{n}(\boldsymbol{s}))dS(\boldsymbol{u})\,dS(\boldsymbol{s})\,d\boldsymbol{\kappa}\Big),\end{aligned} \tag{A.7}$$

where $dS(\boldsymbol{s})$ denotes the infinitesimal surface element that replaces $S(\mathcal{V}\cap T(\boldsymbol{s}))$ in Eq. (A.6).

Equation (A.7) finally yields the closed-form expression (24) of the anisotropic pseudo spectrum $\widehat{J}_L$, which is such that for any Borel set $\mathcal{K}\subset\mathbb{R}^3$, $\int_{\boldsymbol{\kappa}\in\mathcal{K}}\widehat{J}_L(\boldsymbol{\kappa},k)d\boldsymbol{\kappa} = \widehat{\mathcal{J}}_L(\mathcal{K},\overline{V},k)$.

Appendix B.

In this appendix, we prove that function $\boldsymbol{\mathcal{K}}_L(\boldsymbol{k},k)$ defined in Eq. (27) satisfies Eq. (26) asymptotically. In the first place, let us assume that $\forall\boldsymbol{s}\in\partial V$, $k\widehat{\beta}(\boldsymbol{s},k)\in\imath\mathbb{R}$. In this case, the function $\boldsymbol{\mathcal{K}}_L(\boldsymbol{k},k)$ defined in Eq. (27) is real-valued. We then introduce the vector $\boldsymbol{\kappa} = \boldsymbol{\mathcal{K}}_L(\boldsymbol{k},k)\in\mathbb{R}^3$, so that reciprocally, $\boldsymbol{k} = \boldsymbol{\mathcal{K}}_L^{-1}(\boldsymbol{\kappa},k)$. We then note that function $\boldsymbol{k}\mapsto\boldsymbol{\mathcal{K}}_L(\boldsymbol{k},k)-\boldsymbol{k}$ is bounded. Therefore, writing $\|\boldsymbol{k}\|_2\to+\infty$ is equivalent to writing $\|\boldsymbol{\kappa}\|_2\to+\infty$, and $O\left(\frac{1}{\|\boldsymbol{\kappa}\|_2}\right) = O\left(\frac{1}{\|\boldsymbol{k}\|_2}\right)$.

Let us now determine the inverse of the Jacobian matrix $\mathrm{Jac}_{\boldsymbol{\mathcal{K}}_L}(\boldsymbol{k},k)$:

$$\begin{aligned}\mathrm{Jac}_{\boldsymbol{\mathcal{K}}_L^{-1}}(\boldsymbol{\kappa},k) = \ & \boldsymbol{I} - \imath\tfrac{\lambda}{4\pi}\int_{\boldsymbol{s}\in\partial V}\int_{\boldsymbol{u}\in\mathcal{S}(0,1)}\psi'(\boldsymbol{u}^\top\boldsymbol{\kappa},k\,\widehat{\beta}(\boldsymbol{s},k))\boldsymbol{u}\boldsymbol{u}^\top\,\sigma_L(\boldsymbol{u},\boldsymbol{n}(\boldsymbol{s}))\,dS(\boldsymbol{u})\,dS(\boldsymbol{s}) \\ = \ & \boldsymbol{I} + \tfrac{\lambda}{4\pi}\int_{\boldsymbol{s}\in\partial V}\int_{\boldsymbol{u}\in\mathcal{S}(0,1)}\Big(2\pi\,\mathrm{sign}(\mathrm{Im}(k\,\widehat{\beta}(\boldsymbol{s},k))\,\delta\left(\boldsymbol{u}^\top\boldsymbol{\kappa}\right) - \tfrac{\imath}{\boldsymbol{u}^\top\boldsymbol{\kappa}+k\,\widehat{\beta}(\boldsymbol{s},k)} + \tfrac{\imath}{\boldsymbol{u}^\top\boldsymbol{\kappa}-k\,\widehat{\beta}(\boldsymbol{s},k)}\Big) \\ & \times\boldsymbol{u}\boldsymbol{u}^\top\,\sigma_L(\boldsymbol{u},\boldsymbol{n}(\boldsymbol{s}))\,dS(\boldsymbol{u})\,dS(\boldsymbol{s}),\end{aligned} \tag{B.1}$$

where the function $\psi(x,z)$ was defined in Eq. (A.4), and its derivative $\psi'(x,z)$ was expressed in Eq. (A.5). Let us now show that the integral in the last member of Eq. (B.1) is of order $O\left(\frac{1}{\|\boldsymbol{\kappa}\|_2}\right)$. Indeed, we have

$$\begin{aligned} & \left\|\int_{\boldsymbol{u}\in\mathcal{S}(0,1)}\delta(\boldsymbol{u}^\top\boldsymbol{\kappa})\,\boldsymbol{u}\boldsymbol{u}^\top\,\sigma_L(\boldsymbol{u},\boldsymbol{n}(\boldsymbol{s}))\,dS(\boldsymbol{u})\right\|_\infty \\ = & \left\|\tfrac{1}{\|\boldsymbol{\kappa}\|_2}\int_{\boldsymbol{u}\in\mathcal{S}(0,1)\cap\boldsymbol{\kappa}^\perp}\boldsymbol{u}\boldsymbol{u}^\top\,\sigma_L(\boldsymbol{u},\boldsymbol{n}(\boldsymbol{s}))\,dL(\boldsymbol{u})\right\|_\infty = O\left(\tfrac{1}{\|\boldsymbol{\kappa}\|_2}\right),\end{aligned} \tag{B.2}$$

where $dL(\boldsymbol{u})$ denotes the length element on the unit circle $\mathcal{S}(0,1)\cap\boldsymbol{\kappa}^\perp$. In addition,

$$\begin{aligned} & \left\|\int_{\boldsymbol{u}\in\mathcal{S}(0,1)}\left(-\tfrac{\imath}{\boldsymbol{u}^\top\boldsymbol{\kappa}+k\,\widehat{\beta}(\boldsymbol{s},k)} + \tfrac{\imath}{\boldsymbol{u}^\top\boldsymbol{\kappa}-k\,\widehat{\beta}(\boldsymbol{s},k)}\right)\boldsymbol{u}\boldsymbol{u}^\top\,\sigma_L(\boldsymbol{u},\boldsymbol{n}(\boldsymbol{s}))\,dS(\boldsymbol{u})\right\|_\infty \\ \leq \ & \sup_{\boldsymbol{u}\in\mathcal{S}(0,1)}|\sigma_L(\boldsymbol{u},\boldsymbol{n}(\boldsymbol{s}))|\int_{\boldsymbol{u}\in\mathcal{S}(0,1)}\left|\tfrac{2k\,\widehat{\beta}(\boldsymbol{s},k))}{(\boldsymbol{u}^\top\boldsymbol{\kappa})^2-(k\,\widehat{\beta}(\boldsymbol{s},k))^2}\right|dS(\boldsymbol{u}) \\ = \ & \sup_{\boldsymbol{u}\in\mathcal{S}(0,1)}|\sigma_L(\boldsymbol{u},\boldsymbol{n}(\boldsymbol{s}))|\,\tfrac{8\pi\left|k\,\widehat{\beta}(\boldsymbol{s},k))\right|}{\|\boldsymbol{\kappa}\|_2}\int_{v=0}^{+\infty}\tfrac{1}{v^2+\left|k\,\widehat{\beta}(\boldsymbol{s},k)\right|^2}dv \\ = \ & \sup_{\boldsymbol{u}\in\mathcal{S}(0,1)}|\sigma_L(\boldsymbol{u},\boldsymbol{n}(\boldsymbol{s}))|\times\tfrac{4\pi^2}{\|\boldsymbol{\kappa}\|_2} = O\left(\tfrac{1}{\|\boldsymbol{\kappa}\|_2}\right).\end{aligned} \tag{B.3}$$

We have thus proved that the integral in the last member of Eq. (B.1) is of order $O\left(\frac{1}{\|\boldsymbol{\kappa}\|_2}\right)$.

In other respects, note that $\text{Jac}_{\boldsymbol{\mathcal{K}}_L^{-1}}(\boldsymbol{\kappa}, k)$ in Eq. (B.1) is an analytic function of $\boldsymbol{\kappa}$ on $\mathbb{R}^3 \backslash \{\mathbf{0}\}$ (in particular, the integral that is upper bounded in Eq. (B.2) is an analytic function of $\boldsymbol{\kappa}$, for the same reason as that explained in Badeau (2026, Subsection 3 of Appendix B). In addition, Eqs. (B.2) and (B.3) show that asymptotically, i.e., when $\|\boldsymbol{\kappa}\|_2 \to +\infty$, the Jacobian matrix $\text{Jac}_{\boldsymbol{\mathcal{K}}_L^{-1}}(\boldsymbol{\kappa}, k)$ in Eq. (B.1) tends to the identity matrix, thus $\det\left(\text{Jac}_{\boldsymbol{\mathcal{K}}_L^{-1}}(\boldsymbol{\kappa}, k)\right) \to 1$. Consequently, the subset $\mathcal{N}_L$ of $\mathbb{R}^3 \backslash \{\mathbf{0}\}$ where $\det\left(\text{Jac}_{\boldsymbol{\mathcal{K}}_L^{-1}}(\boldsymbol{\kappa}, k)\right) \leq 0$ is bounded. Then, let $\mathcal{D}(\boldsymbol{\mathcal{K}}_L^{-1})$ be largest connected subset of $\mathbb{R}^3 \backslash \mathcal{N}_L$. The domain $\mathcal{D}(\boldsymbol{\mathcal{K}}_L^{-1})$ is the largest open subset of $\mathbb{R}^3 \backslash \{\mathbf{0}\}$, which extends to infinity, where $\det\left(\text{Jac}_{\boldsymbol{\mathcal{K}}_L^{-1}}(\boldsymbol{\kappa}, k)\right) > 0$. Finally, let $\mathcal{D}(\boldsymbol{\mathcal{K}}_L)$ be the image of $\mathcal{D}(\boldsymbol{\mathcal{K}}_L^{-1})$ by $\boldsymbol{\mathcal{K}}_L^{-1}$. The domain $\mathcal{D}(\boldsymbol{\mathcal{K}}_L)$ is such that $\forall \boldsymbol{k} \in \mathcal{D}(\boldsymbol{\mathcal{K}}_L)$, $\det\left(\text{Jac}_{\boldsymbol{\mathcal{K}}_L}(\boldsymbol{k}, k)\right) = \frac{1}{\det\left(\text{Jac}_{\boldsymbol{\mathcal{K}}_L^{-1}}(\boldsymbol{\kappa}, k)\right)} > 0$. Since $\det\left(\text{Jac}_{\boldsymbol{\mathcal{K}}_L^{-1}}(\boldsymbol{\kappa}, k)\right) \to 1$ when $\|\boldsymbol{\kappa}\|_2 \to +\infty$, we deduce that $\det\left(\text{Jac}_{\boldsymbol{\mathcal{K}}_L}(\boldsymbol{k}, k)\right) \to 1$ when $\|\boldsymbol{k}\|_2 \to +\infty$, therefore $\mathcal{D}(\boldsymbol{\mathcal{K}}_L)$ also extends to infinity, and the set $\mathbb{R}^3 \backslash \mathcal{D}(\boldsymbol{\mathcal{K}}_L)$ is bounded.

Therefore, we can conclude that function $\boldsymbol{\mathcal{K}}_L$ is an analytic diffeomorphism from $\mathcal{D}(\boldsymbol{\mathcal{K}}_L)$ to $\mathcal{D}(\boldsymbol{\mathcal{K}}_L^{-1})$. In addition, the determinant of matrix $\text{Jac}_{\boldsymbol{\mathcal{K}}_L^{-1}}(\boldsymbol{\kappa}, k)$ in Eq. (B.1) admits the following first order expansion:

$$\begin{aligned}\det\left(\text{Jac}_{\boldsymbol{\mathcal{K}}_L^{-1}}(\boldsymbol{\kappa}, k)\right) = \; & 1 + \tfrac{\lambda}{4\pi} \int_{\boldsymbol{s} \in \partial V} \int_{\boldsymbol{u} \in \mathcal{S}(0,1)} \Big(2\pi \text{sign}(\text{Im}(k\widehat{\beta}(\boldsymbol{s}, k))\delta(\boldsymbol{u}^\top \boldsymbol{\kappa}) \\ & - \tfrac{\imath}{\boldsymbol{u}^\top \boldsymbol{\kappa} + k\widehat{\beta}(\boldsymbol{s},k)} + \tfrac{\imath}{\boldsymbol{u}^\top \boldsymbol{\kappa} - k\widehat{\beta}(\boldsymbol{s},k)}\Big) \sigma_L(\boldsymbol{u}, \boldsymbol{n}(\boldsymbol{s})) dS(\boldsymbol{u}) dS(\boldsymbol{s}).\end{aligned} \tag{B.4}$$

Finally, if we compare the closed-form expressions of the power spectrum $\widehat{\Gamma}_L(\boldsymbol{k})$ in Eq. (22), the pseudo spectrum $\widehat{J}_L(\boldsymbol{\kappa}, k)$ in Eq. (24), and the determinant $\det\left(\text{Jac}_{\boldsymbol{\mathcal{K}}_L^{-1}}(\boldsymbol{\kappa}, k)\right)$ in Eq. (B.4), we notice that in the three equations, the integrals are of order $O\left(\frac{1}{\|\boldsymbol{\kappa}\|_2}\right)$, and asymptotically we get

$$\widehat{\Gamma}_L(\boldsymbol{\kappa}) \times \det\left(\text{Jac}_{\boldsymbol{\mathcal{K}}_L^{-1}}(\boldsymbol{\kappa}, k)\right) = \widehat{J}_L(\boldsymbol{\kappa}, k). \tag{B.5}$$

In addition, we remark that:

- the truncation to a finite degree L of the series expansion of the directional measure σ over spherical harmonics implies angular smoothing, therefore function $\widehat{\Gamma}_L(\boldsymbol{k})$ is a smooth function of the direction of vector $\boldsymbol{k}$ (more precisely, we explained in Badeau (2026, Subsection 3 of Appendix B) that function $\widehat{\Gamma}_L(\boldsymbol{k})$ is analytic);
- when $\|\boldsymbol{k}\|_2 \to +\infty$, the distance $\|\boldsymbol{\kappa} - \boldsymbol{k}\|_2$ stays bounded as mentioned previously, so the direction of vector $\boldsymbol{\kappa}$ converges to that of vector $\boldsymbol{k}$.

Thus asymptotically, we get $\widehat{\Gamma}_L(\boldsymbol{\kappa}) = \widehat{\Gamma}_L(\boldsymbol{k})$, up to the first order of the asymptotic expansion when $\|\boldsymbol{k}\|_2 \to +\infty$. Therefore, Eq. (B.5) can be rewritten $\widehat{\Gamma}_L(\boldsymbol{k}) \times \det\left(\text{Jac}_{\boldsymbol{\mathcal{K}}_L^{-1}}(\boldsymbol{\kappa}, k)\right) = \widehat{J}_L(\boldsymbol{\kappa}, k)$, and we can finally conclude that Eq. (26) holds in $\mathcal{D}(\boldsymbol{\mathcal{K}}_L)$ as a first order asymptotic expansion.

In other respects, since the three functions $\widehat{\Gamma}_L$, $\widehat{J}_L$ and $\boldsymbol{\mathcal{K}}_L$ are analytic, Eq. (26) still holds by analytic continuation in a mathematical neighborhood of $\mathcal{D}(\boldsymbol{\mathcal{K}}_L)$ in $\mathbb{C}^3$. In the same way, if we no longer assume that $\forall \boldsymbol{s} \in \partial V$, $k\widehat{\beta}(\boldsymbol{s}, k) \in \imath\mathbb{R}$, but only that $k\widehat{\beta}(\boldsymbol{s}, k) \notin \mathbb{R}$, then we note that the three functions $\widehat{\Gamma}_L$, $\widehat{J}_L$ and $\boldsymbol{\mathcal{K}}_L$ are analytic w.r.t both $\boldsymbol{k}$ and $k\widehat{\beta}(\boldsymbol{s}, k)$, therefore Eq. (26) still holds by analytic continuation in a mathematical neighborhood of $\mathcal{D}(\boldsymbol{\mathcal{K}}_L)$ in $\mathbb{C}^3$.

Appendix C.

In this appendix, we derive the spectral representation of the Green's function, which was given in Eq. (32). First, the inverse 3D Fourier transform of the anisotropic pseudo spectrum $\widehat{J}_L(\boldsymbol{\kappa}, k)$ defined in Eq. (24) is a tempered distribution $J_L(\boldsymbol{z}, k)$, which is such that for any analytic function $\psi \in \mathcal{S}(\mathbb{R}^3)$,

$$\left\langle J_L(\boldsymbol{z}, k) \middle| \widehat{\psi}(\boldsymbol{z}) \right\rangle = \int_{\boldsymbol{\kappa} \in \mathbb{R}^3} \psi(\boldsymbol{\kappa})\, \widehat{J}_L(\boldsymbol{\kappa}, k)\, d\boldsymbol{\kappa}. \tag{C.1}$$

Then, because the set $\mathbb{R}^3 \backslash \mathcal{D}(\boldsymbol{\mathcal{K}}_L)$ is bounded (as explained in Appendix B), and because we are working under the high frequency assumption introduced in Sec. 4.2, the integral over $\mathbb{R}^3$ in Eq. (C.1) can be replaced by an integral over $\mathcal{D}(\boldsymbol{\mathcal{K}}_L)$:

$$\left\langle J_L(\boldsymbol{z}, k) \middle| \widehat{\psi}(\boldsymbol{z}) \right\rangle = \int_{\boldsymbol{\kappa} \in \mathcal{D}(\boldsymbol{\mathcal{K}}_L)} \psi(\boldsymbol{\kappa})\, \widehat{J}_L(\boldsymbol{\kappa}, k)\, d\boldsymbol{\kappa}. \tag{C.2}$$

In other words, contrary to Eq. (C.1) that holds exactly, Eq. (C.2) only holds asymptotically (i.e., at high frequency). In other respects, we note from Eq. (27) that $\lim_{\|\boldsymbol{k}\|_2 \to +\infty} \boldsymbol{\mathcal{K}}_L(\boldsymbol{k}, k) - \boldsymbol{k} = \boldsymbol{0}$. Therefore, as we explained in Badeau (2024, Sec. VI C), we can write

$$\left\langle J_L(\boldsymbol{z}, k) \middle| \widehat{\psi}(\boldsymbol{z}) \right\rangle = \int_{\boldsymbol{\kappa} \in \boldsymbol{\mathcal{K}}_L(\mathcal{D}(\boldsymbol{\mathcal{K}}_L), k)} \psi(\boldsymbol{\kappa})\, \widehat{J}_L(\boldsymbol{\kappa}, k)\, d\boldsymbol{\kappa}, \tag{C.3}$$

by analytic continuation in the complex plane of the pseudo spectrum $\widehat{J}_L$ in Eq. (24) and of the analytic function ψ, and by applying Cauchy's integral theorem (Ahlfors, 1979) to the right member of Eq. (C.2).

Then with the change of variable $\boldsymbol{\kappa} = \boldsymbol{\mathcal{K}}_L(\boldsymbol{k}, k)$, Eqs. (26) and (C.3) yield

$$\left\langle J_L(\boldsymbol{z}, k) \middle| \widehat{\psi}(\boldsymbol{z}) \right\rangle = \int_{\boldsymbol{k} \in \mathcal{D}(\boldsymbol{\mathcal{K}}_L)} \psi\left(\boldsymbol{\mathcal{K}}_L(\boldsymbol{k}, k)\right) \widehat{\Gamma}_L(\boldsymbol{k})\, d\boldsymbol{k}. \tag{C.4}$$

In other respects, Eq. (6) shows that

$$J_L(\boldsymbol{z}, k) = \left(\Delta + 4\pi^2 k^2\right)^2 J_G(\boldsymbol{z}, k), \tag{C.5}$$

where $J_G(\boldsymbol{z}, k)$ denotes the PCF of the pseudo-stationary Green's function $G(\boldsymbol{x}, \boldsymbol{x}_0, k)$, which is a tempered distribution, like $J_L(\boldsymbol{z}, k)$. We deduce from Eqs. (C.4) and (C.5) that

$$\left\langle J_G(\boldsymbol{z}, k) \middle| \left(\Delta + 4\pi^2 k^2\right)^2 \widehat{\psi}(\boldsymbol{z}) \right\rangle = \left\langle J_L(\boldsymbol{z}, k) \middle| \widehat{\psi}(\boldsymbol{z}) \right\rangle = \int_{\boldsymbol{k} \in \mathcal{D}(\boldsymbol{\mathcal{K}}_L)} \psi\left(\boldsymbol{\mathcal{K}}_L(\boldsymbol{k}, k)\right) \widehat{\Gamma}_L(\boldsymbol{k})\, d\boldsymbol{k}. \tag{C.6}$$

Therefore, the tempered distribution $J_G(\boldsymbol{z},k)$ can equivalently be written as a function:

$$J_G(\boldsymbol{z},k) = \int_{\boldsymbol{k}\in\mathcal{D}(\boldsymbol{\mathcal{K}}_L)} \frac{e^{2\imath\pi\boldsymbol{\mathcal{K}}_L(\boldsymbol{k},k)^\top \boldsymbol{z}}}{\left(4\pi^2(\boldsymbol{\mathcal{K}}_L(\boldsymbol{k},k)^\top\boldsymbol{\mathcal{K}}_L(\boldsymbol{k},k)-k^2)\right)^2}\,\widehat{\Gamma}_L(\boldsymbol{k})d\boldsymbol{k}, \tag{C.7}$$

which indeed satisfies Eq. (C.6):

$$\begin{aligned}
&\left\langle J_G(\boldsymbol{z},k)\middle| \left(\Delta+4\pi^2k^2\right)^2\widehat{\psi}(\boldsymbol{z})\right\rangle\\
=\ & \int_{\boldsymbol{z}\in\mathbb{R}^3}\left(\Delta+4\pi^2k^2\right)^2\widehat{\psi}(\boldsymbol{z})\int_{\boldsymbol{k}\in\mathcal{D}(\boldsymbol{\mathcal{K}}_L)}\frac{e^{2\imath\pi\boldsymbol{\mathcal{K}}_L(\boldsymbol{k},k)^\top \boldsymbol{z}}}{\left(4\pi^2(\boldsymbol{\mathcal{K}}_L(\boldsymbol{k},k)^\top\boldsymbol{\mathcal{K}}_L(\boldsymbol{k},k)-k^2)\right)^2}\widehat{\Gamma}_L(\boldsymbol{k})d\boldsymbol{k}\,d\boldsymbol{z}\\
=\ & \int_{\boldsymbol{k}\in\mathcal{D}(\boldsymbol{\mathcal{K}}_L)}\widehat{\Gamma}_L(\boldsymbol{k})\left(\int_{\boldsymbol{z}\in\mathbb{R}^3}\widehat{\psi}(\boldsymbol{z})\frac{\left(\Delta+4\pi^2k^2\right)^2e^{2\imath\pi\boldsymbol{\mathcal{K}}_L(\boldsymbol{k},k)^\top \boldsymbol{z}}}{\left(4\pi^2(\boldsymbol{\mathcal{K}}_L(\boldsymbol{k},k)^\top\boldsymbol{\mathcal{K}}_L(\boldsymbol{k},k)-k^2)\right)^2}d\boldsymbol{z}\right)d\boldsymbol{k}\\
=\ & \int_{\boldsymbol{k}\in\mathcal{D}(\boldsymbol{\mathcal{K}}_L)}\widehat{\Gamma}_L(\boldsymbol{k})\left(\int_{\boldsymbol{z}\in\mathbb{R}^3}\widehat{\psi}(\boldsymbol{z})e^{2\imath\pi\boldsymbol{\mathcal{K}}_L(\boldsymbol{k},k)^\top \boldsymbol{z}}d\boldsymbol{z}\right)d\boldsymbol{k}\\
=\ & \int_{\boldsymbol{k}\in\mathcal{D}(\boldsymbol{\mathcal{K}}_L)}\psi\left(\boldsymbol{\mathcal{K}}_L(\boldsymbol{k},k)\right)\widehat{\Gamma}_L(\boldsymbol{k})d\boldsymbol{k}.
\end{aligned}$$

Then, if we assume that the spectral representation of the random process $G(\boldsymbol{x},\boldsymbol{x}_0,k)$ is a distortion of the spectral representation in Eq. (19) that we obtained in the case of Neumann's boundary condition, we get Eq. (32). Indeed, the PCF of the Green's function $G(\boldsymbol{x},\boldsymbol{x}_0,k)$ defined in Eq. (32) does satisfy Eq. (C.7):

$$\begin{aligned}
&\operatorname{cov}[G(\boldsymbol{x}_1,\boldsymbol{x}_0,k),\overline{G(\boldsymbol{x}_2,\boldsymbol{x}_0,k)}]\\
=\ & \int_{\boldsymbol{k}\in\mathcal{D}(\boldsymbol{\mathcal{K}}_L)}\int_{\boldsymbol{s}\in\overline{V}}\frac{e^{2\imath\pi\boldsymbol{\mathcal{K}}_L(\boldsymbol{k},k)^\top(\boldsymbol{x}_1-\boldsymbol{s})}}{4\pi^2(\boldsymbol{\mathcal{K}}_L(\boldsymbol{k},k)^\top\boldsymbol{\mathcal{K}}_L(\boldsymbol{k},k)-k^2)}\frac{e^{-2\imath\pi\boldsymbol{\mathcal{K}}_L(\boldsymbol{k},k)^\top(\boldsymbol{x}_2-\boldsymbol{s})}}{4\pi^2(\boldsymbol{\mathcal{K}}_L(\boldsymbol{k},k)^\top\boldsymbol{\mathcal{K}}_L(\boldsymbol{k},k)-k^2)}d\widehat{\Lambda}_L(\boldsymbol{k},\boldsymbol{s})\\
=\ & \int_{\boldsymbol{k}\in\mathcal{D}(\boldsymbol{\mathcal{K}}_L)}\frac{e^{2\imath\pi\boldsymbol{\mathcal{K}}_L(\boldsymbol{k},k)^\top(\boldsymbol{x}_1-\boldsymbol{x}_2)}}{\left(4\pi^2(\boldsymbol{\mathcal{K}}_L(\boldsymbol{k},k)^\top\boldsymbol{\mathcal{K}}_L(\boldsymbol{k},k)-k^2)\right)^2}d\widehat{\Lambda}_L(\boldsymbol{k},\overline{V}) = J_G(\boldsymbol{x}_1-\boldsymbol{x}_2,k),
\end{aligned}$$

due to Eq. (23).

Appendix D.

In this appendix, we derive the closed-form expression of the causal source response p introduced in Eq. (3). Substituting Eq. (32) into Eq. (5) yields

$$\dot{g}(\boldsymbol{x},\boldsymbol{x}_0,t) = \mu_{\dot{g}}(t) - c^2\int_{\boldsymbol{k}\in\mathcal{D}(\boldsymbol{\mathcal{K}}_L)}\int_{\boldsymbol{s}\in\overline{V}}\int_{f\in\mathbb{R}}\frac{2\imath\pi f\,e^{2\imath\pi\boldsymbol{\mathcal{K}}_L(\boldsymbol{k},\frac{f}{c})^\top(\boldsymbol{x}-\boldsymbol{s})}}{4\pi^2(f^2-c^2\boldsymbol{\mathcal{K}}_L(\boldsymbol{k},\frac{f}{c})^\top\boldsymbol{\mathcal{K}}_L(\boldsymbol{k},\frac{f}{c}))}\,e^{2\imath\pi ft}df\,d\widehat{\xi}_L(\boldsymbol{k},\boldsymbol{s}), \tag{D.1}$$

with

$$\mu_{\dot{g}}(t) = \int_{f\in\mathbb{R}}\mu_G(\tfrac{f}{c})\,2\imath\pi f\,e^{2\imath\pi ft}df = \tfrac{\lambda c^2}{2}\operatorname{sign}(t). \tag{D.2}$$

Then, due to Eq. (28), the equation $\kappa^2 = \boldsymbol{\mathcal{K}}_L(\boldsymbol{k},\kappa)^\top\boldsymbol{\mathcal{K}}_L(\boldsymbol{k},\kappa)$ admits two roots: one root at $\kappa=\kappa_L(\boldsymbol{k})$ (where $\kappa_L(\boldsymbol{k})$ was defined in Eq. (33)), with both non-negative real and imaginary parts, and another root at $\kappa = -\overline{\kappa_L(\boldsymbol{k})}$, with non-positive real part and non-negative imaginary part. Therefore, the equation $f^2 = c^2\boldsymbol{\mathcal{K}}_L(\boldsymbol{k},\frac{f}{c})^\top\boldsymbol{\mathcal{K}}_L(\boldsymbol{k},\frac{f}{c})$ admits two solutions $f=c\kappa_L(\boldsymbol{k})$ and $f=-c\overline{\kappa_L(\boldsymbol{k})}$, which are both in the upper half complex plane.

By applying the residue theorem (Ahlfors, 1979) to Eq. (D.1), we thus get:

$$\dot{g}(\boldsymbol{x},\boldsymbol{x}_0,t) = \mu_{\dot{g}}(t) + c^2 H(t)\mathrm{Re}\Big(\int_{\boldsymbol{k}\in\mathcal{D}(\boldsymbol{\mathcal{K}}_L)} \int_{\boldsymbol{s}\in\overline{V}} e^{2\imath\pi\left(\boldsymbol{\kappa}_L(\boldsymbol{k})^\top(\boldsymbol{x}-\boldsymbol{s})+c\,\kappa_L(\boldsymbol{k})t\right)} d\widehat{\xi}_L(\boldsymbol{k},\boldsymbol{s})\Big), \quad \text{(D.3)}$$

where the real part comes from Eqs. (28) and (29), and from the change of variable $\boldsymbol{k}\to-\boldsymbol{k}$.

The causal source response p introduced in Eq. (3) is related to $\dot{g}$ by adding the constant term $\frac{\lambda c^2}{2}$, which is a solution to the homogeneous wave equation [Eq. (1)]:

$$p(\boldsymbol{x},\boldsymbol{x}_0,t) = \dot{g}(\boldsymbol{x},\boldsymbol{x}_0,t) + \tfrac{\lambda c^2}{2}. \quad \text{(D.4)}$$

By substituting Eq. (D.3) into Eq. (D.4), we finally get Eqs. (35) and (36). Then, based on Eq. (36), the ACF Γ_q of the random process q defined in Eq. (15) is a tempered distribution, so that $\forall\psi(f)\in\mathcal{S}(\mathbb{R})$ such that $\psi(0)=0$ at $f=0$ [4],

$$\begin{aligned}&\Big\langle \Gamma_q(\boldsymbol{x}_1,\boldsymbol{x}_2,\boldsymbol{x}_0,t+\tfrac{\tau}{2},t-\tfrac{\tau}{2})\Big|\widehat{\psi}(\tau)\Big\rangle\\
=\;& \tfrac{c^4}{4}\int_{\boldsymbol{k}\in\mathcal{D}(\boldsymbol{\mathcal{K}}_L)}\int_{\boldsymbol{s}\in\overline{V}} e^{-4\pi c\mathrm{Im}(\kappa_L(\boldsymbol{k}))t}\Big(e^{2\imath\pi\left(\boldsymbol{\kappa}_L(\boldsymbol{k})^\top(\boldsymbol{x}_1-\boldsymbol{s})-\boldsymbol{\kappa}_L(\boldsymbol{k})^H(\boldsymbol{x}_2-\boldsymbol{s})\right)}\psi(c\mathrm{Re}(\kappa_L(\boldsymbol{k})))\\
&+e^{-2\imath\pi\left(\boldsymbol{\kappa}_L(\boldsymbol{k})^H(\boldsymbol{x}_1-\boldsymbol{s})-\boldsymbol{\kappa}_L(\boldsymbol{k})^\top(\boldsymbol{x}_2-\boldsymbol{s})\right)}\psi(-c\mathrm{Re}(\kappa_L(\boldsymbol{k})))\Big)d\widehat{\Lambda}_L(\boldsymbol{k},\boldsymbol{s}),\end{aligned} \quad \text{(D.5)}$$

where we have used Eq. (20), and where the spectral measure $\widehat{\Lambda}_L(\mathcal{K},\mathcal{V})$ was defined in Eq. (21).

Appendix E.

In this appendix, we derive the asymptotic expansion of the cross-Wigner distribution of the random process q, which was expressed in Eq. (36). By substituting Eq. (D.5) into Eq. (16) [5], we get

$$\begin{aligned}W_q(\boldsymbol{x}_1,\boldsymbol{x}_2,\boldsymbol{x}_0,f,t) =\;& \tfrac{c^3}{4}\int_{\boldsymbol{l}\in\mathcal{D}(\boldsymbol{\mathcal{K}}_L)}\delta\left(\mathrm{Re}(\kappa_L(\boldsymbol{l}))-\tfrac{f}{c}\right)e^{-4\pi c\mathrm{Im}(\kappa_L(\boldsymbol{l}))t}\\
&\times\int_{\boldsymbol{s}\in\overline{V}} e^{2\imath\pi\left(\boldsymbol{\kappa}_L(\boldsymbol{l})^\top(\boldsymbol{x}_1-\boldsymbol{s})-\boldsymbol{\kappa}_L(\boldsymbol{l})^H(\boldsymbol{x}_2-\boldsymbol{s})\right)}d\widehat{\Lambda}_L(\boldsymbol{l},\boldsymbol{s}),\end{aligned} \quad \text{(E.1)}$$

where $\kappa_L(\boldsymbol{l})\in\mathbb{C}$ denotes the wave numbers distortion defined in Eq. (38), $\boldsymbol{\kappa}_L(\boldsymbol{l})\in\mathbb{C}^3$ denotes the wave vectors distortion defined in Eq. (37), and the spectral measure $\widehat{\Lambda}_L(\mathcal{K},\mathcal{V})$ was defined in Eq. (21).

If we assume that function $\boldsymbol{k}\mapsto(\mathrm{Re}\boldsymbol{\kappa}_L)^{-1}(\boldsymbol{k})$ is continuously differentiable[6] on $\mathcal{S}(0,\frac{f}{c})$, then with the change of variable $\boldsymbol{k}=\mathrm{Re}(\boldsymbol{\kappa}_L(\boldsymbol{l}))$ in Eq. (E.1), and by noting that asymptotically $\|\boldsymbol{k}\|_2=\mathrm{Re}(\kappa_L(\boldsymbol{l}))$, we obtain Eq. (43), where $\widehat{\Gamma}_{\boldsymbol{\kappa}_L}(\boldsymbol{x},\boldsymbol{k})$ was defined in Eq. (45).

[4] We can assume that $\psi(0)=0$ without loss of generality, because the theory holds at high frequency, as explained in Sec. 4.2. This assumption permitted us to simplify the expression of the right member in Eq. (D.5).

[5] To derive Eq. (E.1), Eq. (D.5) can be applied to any sequence of Schwartz functions that converges in the sense of distributions to $\psi(\xi)=\delta(\xi-f)$, so that $\widehat{\psi}(\tau)=e^{-\imath 2\pi f\tau}$.

[6] Function $\boldsymbol{k}\mapsto(\mathrm{Re}\boldsymbol{\kappa}_L)^{-1}(\boldsymbol{k})$ is discontinuous on $\mathcal{S}(0,k)$ if the sign of function $k\mapsto\mathrm{Im}\left(\widehat{\beta}(\boldsymbol{s},k)\right)$ changes at k, jointly on a set of points $\boldsymbol{s}$ of non-zero surface measure on the boundary ∂V; otherwise, $\boldsymbol{k}\mapsto(\mathrm{Re}\boldsymbol{\kappa}_L)^{-1}(\boldsymbol{k})$ is continuously differentiable on $\mathcal{S}(0,k)$ if function $k\mapsto\widehat{\beta}(\boldsymbol{s},k)$ is continuously differentiable at k.

If in addition we assume that $\frac{d\widehat{\beta}(\boldsymbol{s},k)}{dk} = o(\frac{1}{k})$, then Eq. (41) yields the following first order asymptotic expansion:

$$\det\left(\mathrm{Jac}_{\mathrm{Re}\,\boldsymbol{\kappa}_L}(\boldsymbol{k})\right) = 1 - \frac{\lambda}{\|\boldsymbol{k}\|_2}\int_{\boldsymbol{s}\in\partial V}\int_{\boldsymbol{u}\in\mathcal{S}(0,1)} \left(\frac{(\boldsymbol{u}^\top\boldsymbol{k})^2-\|\boldsymbol{k}\|_2^2}{2\pi}\,\mathrm{Im}\left(\frac{\widehat{\beta}(\boldsymbol{s},\|\boldsymbol{k}\|_2)}{(\boldsymbol{u}^\top\boldsymbol{k})^2-\|\boldsymbol{k}\|_2^2\widehat{\beta}(\boldsymbol{s},\|\boldsymbol{k}\|_2)^2}\right) + \frac{\mathrm{sign}(\mathrm{Im}(\widehat{\beta}(\boldsymbol{s},\|\boldsymbol{k}\|_2))\delta\left(\frac{\boldsymbol{u}^\top\boldsymbol{k}}{\|\boldsymbol{k}\|_2}\right)}{2}\right)\sigma_L(\boldsymbol{u},\boldsymbol{n}(\boldsymbol{s}))dS(\boldsymbol{u})dS(\boldsymbol{s}). \tag{E.2}$$

When $\|\boldsymbol{k}\|_2 \to +\infty$, Eqs. (E.2) and (46) show that asymptotically, $(\mathrm{Re}\,\boldsymbol{\kappa}_L)^{-1}(\boldsymbol{k})$ can be replaced by $\boldsymbol{k}$ in Eq. (45), which yields

$$\widehat{\Gamma}_{\boldsymbol{\kappa}_L}(\boldsymbol{x},\boldsymbol{k}) = \int_{\boldsymbol{s}\in\overline{V}} e^{-4\pi\mathrm{Im}(\boldsymbol{\kappa}_L(\boldsymbol{k}))^\top(\boldsymbol{x}-\boldsymbol{s})}\frac{d\widehat{\Lambda}_L^0(\boldsymbol{k},\boldsymbol{s})}{\left|\det\left(\mathrm{Jac}_{\mathrm{Re}\,\boldsymbol{\kappa}_L}(\boldsymbol{k})\right)\right|}. \tag{E.3}$$

Finally, by susbstituting Eqs. (E.2) and (46) into Eq. (E.3), we get Eq. (47), where we have used the identity $\delta\left(\boldsymbol{u}^\top\boldsymbol{k}\right) = \frac{1}{\|\boldsymbol{k}\|_2}\delta\left(\frac{\boldsymbol{u}^\top\boldsymbol{k}}{\|\boldsymbol{k}\|_2}\right)$, and we have neglected second order terms.

References

Ahlfors, L. (**1979**). *Complex Analysis* (McGraw-Hill, New York, NY).

Al-Gwaiz, M. A. (**2008**). Springer Undergraduate Mathematics Series *Sturm-Liouville Theory and its Applications* (Springer, London, UK).

Alary, B. (**2021**). "Analysis and synthesis of directional reverberation," Ph.D. thesis, Aalto University, Aalto, Finland.

Alary, B., Politis, A., and Bilbao, S. (**2024**). "Designing directional reverberators for spatial sound reproduction," in *Proceedings of the AES 5th International Conference on Audio for Virtual and Augmented Reality*, Redmond, WA, pp. 1–4.

Alary, B., Politis, A., Schlecht, S., and Välimäki, V. (**2019**). "Directional feedback delay network," Journal of the Audio Engineering Society **67**(10), 752–762.

Arana-Herrera, F., Chaika, J., and Forni, G. (**2025**). "Weak mixing in rational billiards," Annals of Mathematics `arxiv.org/abs/2410.11117`.

Arendt, W., Nittka, R., Peter, W., and Steiner, F. (**2009**). "Weyl's law: Spectral properties of the Laplacian in mathematics and physics," in *Mathematical Analysis of Evolution, Information, and Complexity* (Wiley-VCH, Weinheim, Germany), Chap. 1, pp. 1–71.

Arnold, V. I., and Avez, A. (**1989**). *Ergodic problems of classical mechanics* (Addison-Wesley, Boston, MA).

Badeau, R. (**2024**). "Statistical wave field theory," J. Acoust. Soc. Am. **156**(1), 573–599.

Badeau, R. (**2025**a). "On the spectral decomposition of the complex Robin Laplacian," J. Acoust. Soc. Am. **158**(1), 838–848.

Badeau, R. (**2025**b). "Statistical wave field theory: Curvature term," J. Acoust. Soc. Am. **157**(3), 1650–1664.

Badeau, R. (**2025**c). "Statistical wave field theory: Special polyhedra," J. Acoust. Soc. Am. **157**(3), 2263–2278.

Badeau, R. (**2026**). "Statistical wave field theory: Anisotropic wave fields under Neumann's boundary condition," J. Acoust. Soc. Am. **159**(3), 2265–2280.

Balian, R., and Bloch, C. (**1970**). "Distribution of eigenfrequencies for the wave equation in a finite domain: I. Three-dimensional problem with smooth boundary surface," Ann. Phys. **60**(2), 401–447.

Balian, R., and Bloch, C. (**1972**). "Distribution of eigenfrequencies for the wave equation in a finite domain: III. Eigenfrequency density oscillations," Ann. Phys. **69**(1), 76–160.

Berzborn, M., and Vorländer, M. (**2021**). "Directional sound field decay analysis in performance spaces," Building Acoustics **28**(3), 249–263.

Bilbao, S., and Alary, B. (**2024**). "Directional reverberation time and the image source method for rectangular parallelepipedal rooms," J. Acoust. Soc. Am. **155**(2), 1343–1352.

Brack, M., and Bhaduri, R. (**1997**). *Semiclassical Physics* (Addison-Wesley, Boston, MA).

Cohen, L. (**1989**). "Time-frequency distributions–A review," Proc. IEEE **77**(7), 941–981.

Cook, R. K., Waterhouse, R., Berendt, R., Edelman, S., and Thompson, M. (**1955**). "Measurement of correlation coefficients in reverberant sound fields," J. Acoust. Soc. Am. **27**(6), 1072–1077.

Courant, R., and Hilbert, D. (**2004**). "Special functions defined by eigenvalue problems," in *Methods of Mathematical Physics* (Wiley-VCH, Weinheim, Germany), Chap. 7, pp. 466–549.

Drechsler, S. (**2012**). "The anisotropic reverberation model (ARM) - a simplified method to calculate the sound energy decay and derived properties," in *Proceedings of the 41st International Congress and Exposition on Noise Control Engineering (INTER-NOISE)*, pp. 1–11.

Drechsler, S., and Stephenson, U. M. (**2012**). "A calculation model for anisotropic reverberation with specular and diffuse reflections," in *Proceedings of the DAGA 2012 annual conference on acoustics*, pp. 605–606.

Eyring, C. F. (**1930**). "Reverberation time in 'dead' rooms," J. Acoust. Soc. Am. **1**(2A), 217–241.

Götz, G., Schlecht, S. J., and Pulkki, V. (**2023**). "Common-slope modeling of late reverberation," IEEE/ACM Transactions on Audio, Speech, and Language Processing **31**, 3945–3957.

Joyce, W. B. (**1975**). "Sabine's reverberation time and ergodic auditoriums," J. Acoust. Soc. Am. **58**(3), 643–655.

Joyce, W. B. (**1978**). "Exact effect of surface roughness on the reverberation time of a uniformly absorbing spherical enclosure," J. Acoust. Soc. Am. **64**(5), 1429–1436.

Kanev, N. G. (**2012**). "Sound decay in a rectangular room with impedance walls," Acoustical Physics **58**(5), 603–609.

Kuttruff, H. (**2014**). *Room Acoustics, 5th ed.* (CRC Press, Boca Raton, FL), pp. 1–374.

Meyer-Kahlen, N., and Schlecht, S. J. (**2024**). "Directional distribution of the pseudo intensity vector in anisotropic late reverberation," J. Acoust. Soc. Am. **155**(2), 1515–1526.

Mironov, M. A., and Pislyakov, V. V. (**2002**). "One-dimensional acoustic waves in retarding structures with propagation velocity tending to zero," Acoustical Physics **48**(3), 347–352.

Moorer, J. A. (**1979**). "About this reverberation business," Computer Music Journal **3**(2), 13–28.

Morse, P. M., and Ingard, K. U. (**1968**). *Theoretical acoustics* (McGraw-Hill, New York).

Nolan, M., Fernandez-Grande, E., Brunskog, J., and Jeong, C.-H. (**2018**). "A wavenumber approach to quantifying the isotropy of the sound field in reverberant spaces," J. Acoust. Soc. Am. **143**(4), 2514–2526.

Pelat, A., Gautier, F., Conlon, S. C., and Semperlotti, F. (**2020**). "The acoustic black hole: A review of theory and applications," Journal of Sound and Vibration **476**(115316).

Polack, J.-D. (**1988**). "La transmission de l'énergie sonore dans les salles (*The transmission of sound energy in rooms*)," Ph.D. thesis, Université du Maine, Le Mans, France.

Polack, J.-D. (**1992**). "Modifying chambers to play billiards: the foundations of reverberation theory," Acta Acust. united Acust. **76**(6), 257–272.

Polack, J.-D. (**2025**). "Revisiting reverberation," Acta Acustica **9**(30), 1–19.

Prinn, A. G., and Badeau, R. (**2026**). "Verification of reverberation time predictions derived from the statistical wave field theory," Applied Acoustics **250**, 111337.

Schroeder, M. R. (**1962**). "Frequency-correlation functions of frequency responses in rooms," J. Acoust. Soc. Am. **34**(12), 1819–1823.

Sieber, M., Primack, H., Smilansky, U., Ussishkin, I., and Schanz, H. (**1995**). "Semiclassical quantization of billiards with mixed boundary conditions," Journal of Physics A: Mathematical and General **28**(17), 5041–5078.

Tabachnikov, S. (**1995**). Panoramas et synthèses (*Panoramas and overviews*) *Billiards* (Société mathématique de France, Paris, France).

Weyl, H. (**1911**). "Ueber die asymptotische verteilung der eigenwerte (*On the asymptotic distribution of eigenvalues*)," Nachr. von der Gesellschaft der Wissenschaften zu Göttingen, Mathematisch-Physikalische Klasse **1911**, 110–117.

Xu, Q., Shen, X., Peng, P., Loh, T. H., and Huang, Y. (**2022**). "Alternative definitions of the field anisotropy in a reverberation chamber," in *Proceedings of the 2022 3rd URSI Atlantic and Asia Pacific Radio Science Meeting (AT-AP-RASC)*, pp. 1–4.